UNIVERSITY OF OSLO
Department of Informatics

A Foveated AER Imager Chip

Master thesis

Mehdi Azadmehr

June 2005

ABSTRACT

This thesis presents a foveated imager chip, an imager inspired by the retina in the human eye. The imager shares some functionalities of the retina, with sharp vision in the centre and motion detection in the periphery. To achieve this we use two types of pixels, static pixels emulating the cones and more space consuming dynamic pixels emulating the rods. Inspired by the neurons of biological nervous systems, they emit short voltage pulses, the static pixels with a frequency proportional to light intensity, the dynamic pixels whenever they detect a relative change in irradiance. The pulses are transmitted off-chip by the Address Event Representation (AER), a communication protocol that emulates the behavior of the point-to-point connection in the nervous system.
Using the nervous system as model for circuit design offered many advantages compared to digital cameras, such as compactness, low latency, etc.

Preface

This thesis is the result of my study for the master degree in Microelectronic at the department of informatics, university of Oslo. I started this work spring 2003 and concluded my research spring 2005.
My fascination for the biology, especially the human brain and the nervous system was the main reason for choosing this project. I personally wanted to find out how good an electronic system could match biology. I felt the human retina was a good research object.
During this project I met a lot of challenges, such as keeping deadlines, understanding the biology, but I feel that in the long run I learned a lot and the work became more and more exiting as the puzzles fitted.

This thesis is divided into 4 chapters:
Chapter 1, is the introduction, in this chapter some background information about the biology is presented.
In chapter 2, called A FOVEATED AER IMAGER, the imager is described. The pixels are presented in block diagram and a description of the communication system is presented.
Chapter 3, called implementation, is the description of circuits and the test results. In the beginning of this chapter we describe the test method used and then the schematic of all the circuits are presented followed be the measurements.
Chapter 4 Presents the conclusions and a few proposals for further work.
Based on the project's content we decided to call this thesis, A AER foveated Imager. This project is a supported by a bigger project called Caviar.
A paper based on the result from this project is published at the IEEE conference iscas 2005 in Kobe, Japan.

Oslo, May 2005.

Mehdi Azadmehr

Acknowledgements

I would like to thank all the people that provided me with different types of support. First and foremost I will thank my supervisor Philipp Häfliger for his tremendous support through the whole project, for his guidance and for being available all the time.
I will also thank Jens Petter Abrahamsen for sharing his experiences with me, Omid Mirmotahari and Dag T. Wisland, for assisting me with all my technical difficulties, the Neuromorphic research group and all my fellow students.
I am also grateful to my family for their support all the way, my fiancé for being patient with me in times when I spend all my time in the laboratory trying to keep the deadlines.

The author gratefully acknowledges permission for the reproduction of illustrations, tables and data from the following persons:

Neoromorft kamera by Jens Petter Abrahamsen.

Lecture notes in Neuromorphic electronic by Philipp Häfliger.

Software created by Phillip Häfliger and Mehdi Azadmehr, revised and used for the test.

Multi-Level Static Memory for On-Chip Learning by Håvard Kolle Riis.

Table of contents

1. Introduction

Electronics has undergone a tremendous development in the last decades, from simple circuits made of a few radio tubes in labs to computers containing millions of transistors capable of performing different multimedia applications, solving difficult mathematical equations, etc. However digital systems are facing certain limitation in for example down scaling and power dissipation, at the same time that computational demands are increasing, driven by applications like recognizing, learning, navigation. A possibility to meet these demands would be to move away from the numeric digital systems and exploring other areas, for example the biologically inspired circuits.

The human nervous system, including the brain and the sensory part, has been developed and tested for millions of years by Mother Nature resulting in a processing power that is superior to the most modern digital computers available today. Many of the tasks that researchers struggle to implement into electronic digital systems, like navigation, and learning have been solved by the biology in most clever manner.
The processing power in the biology has attracted the interest of the researchers, and has resulted into extensive effort to emulate it into electronic systems. Already in early fifties a models of an axon was presented by Hodgkin and Huxley [1] and in late eighties, circuits like the I&F [2] circuit by Mead and The Silicon Neuron [3] that emulated the behavior of a single neuron were presented. The effort to imitate the functionality of the brain and the nervous system and implement these systems into electronic circuits has resulted in the research area first time referred to as neuromorphic electronics by Mead.
The neuromorphic researcher tries to take advantage of mixing the best from the biology and the digital and analog world to create smart systems that are more sophisticated and efficient than each of them alone. To achieve this, the Neuromorphic researcher must learn about the biology, the digital and the analog world, and understand the weakness and strength of each system.

Neuromorphic electronics have proven itself as an important research area and has become one of the main sessions in international Conferences like IEEE ISCAS and others. Also the interest for the neuromorphic electronics is increasing as we learn more about the biology and become more experienced in the field.
For example CAVIAR, an international neuromorphic project involving several research organizations, among them University of Oslo is supported by the EU's 5th framework. Caviar has the aim of developing neuromorphic circuits and systems and good results have been presented including some learning circuits and visual circuits etc. The foveated imager presented in this thesis is a typical Neuromorphic circuit. In our imager we use the idea of local calculation, a system inspired by the human eye, resulting in power conservation, low latency and compactness of our system.

1.1 Biology

To be able to design and understand Neuromorphic circuits, one has to have some understanding about the way neurons communicate and calculate. In this section we are going to present some basic information about how neurons work and send information using action potential (AP). We also have included a short description of the human eye and the sensoric cells in the retina at the end of this section.

1.1.1 Neurons

Nerve cells, also called Neurons, form the computation and communication system in our body. They are numbered to 10^{11} neurons, mostly concentrated in the brain. Each nerve cell has, in addition to the soma (cell body), lengthy protrusions called dendrites and axons and connection sites with other neurons called synapses. See figure 1.1

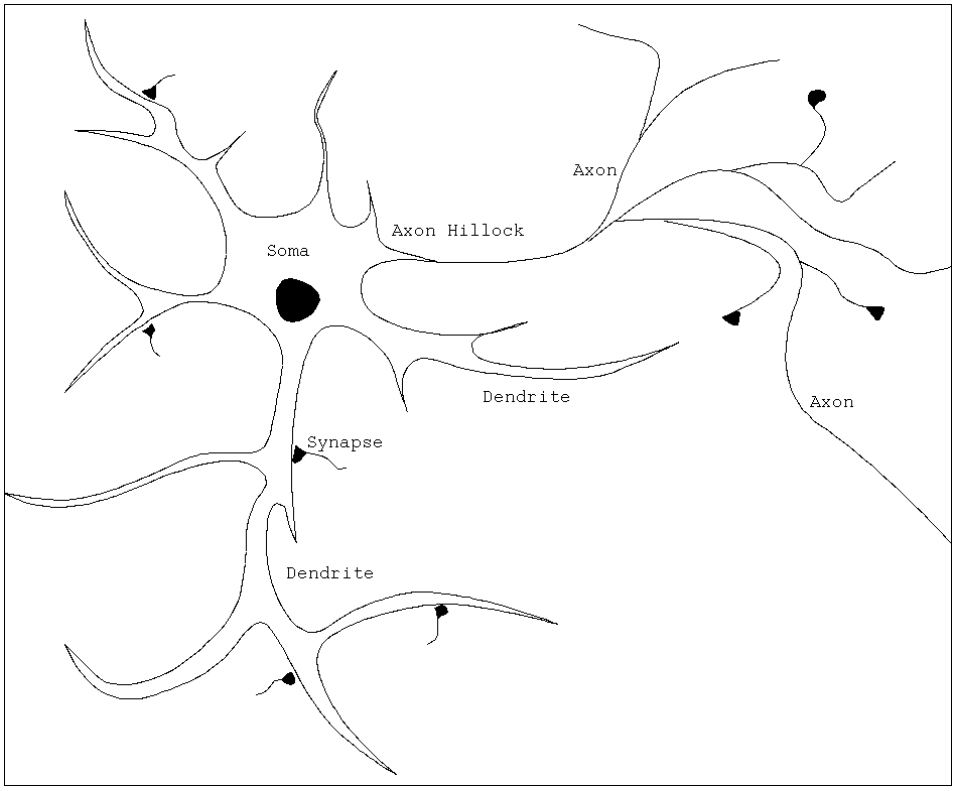

Figure 1.1

The cell body is involved in the main metabolic functions of the cell and their size varies from 4 μm to 100 μm in diameter**.** The dendrites are responsible for receiving signals and conducting them to the soma. The axon is the portion of the neuron that is responsible for the passing of the cellular message from the neuron to either other neurons, or neural receptors [4]. Some axons can be up to 1m long. A synapse is the place where two neurons join in such a way that a signal can be transmitted from one to the other.
The typical type of synapse is the one in which the axon of one neuron activates a second neuron, usually making a synapse with one of its dendrites or with the cell body [5] [6].
Neuron in our body and brain are connected to several other neurons in a three dimensional structure and one neuron can connect to another neuron through several synapses. The synapses have different weights (strengths), meaning that they affect the targeting neuron by different strengths. Input to certain synapses can make a neuron fire an AP, whereas inputs to others only show a minimal or no effect. These synaptic weights serve a main purposes in our brain; they act as codes to store information in the brain (learning) [7].

1.1.2 AP

APs are electric pulses with fixed amplitude of ca 100mV, with a resting potential of -70 mV relative to the outside.
The APs reach a peak of approximately 30 mV and a have duration of approximately 1ms. A typical AP is shown in figure 1.2.

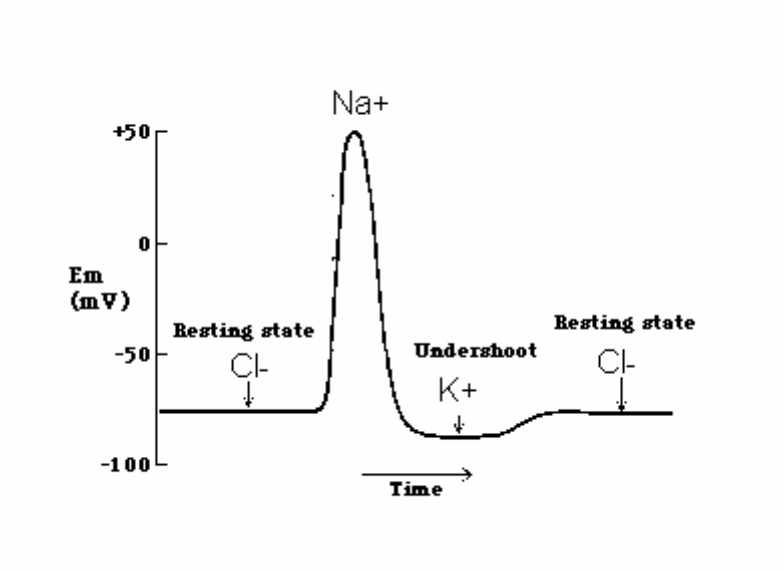

Figure 1.2

Sequential changes in the permeability of the membrane to positive sodium (Na+) ions and potassium (K^+) ions produce electrical signals called action potentials.

Action potentials are caused by an exchange of ions across the neuron membrane due to effect from other neurons as post synaptic current (PSC) on the cell membrane [2]. The receiving neuron integrates the post synaptic current (PSC) through an electrochemical process and fires an AP, if the gathered charge on its body reaches a threshold of approximately -55 mV.
When a neuron fires, it takes about 1.5 milliseconds for a neuron to return to its resting potential during which time it cannot send nerve impulses. This is called the refractory period. There are no grades of nerve impulses - an action potential will either be released or it won't be, and all action potentials are of the same size. [8], [9].
Studies on neurons show that maximum firing rate of a neuron is around 100Hz with a maximum speeds of 160 m/525 ft per second, although many are much slower [10].

Until recently one thought that the only **coding mechanism** in the nerve system, is the firing rate of AP's, or their frequency, but later researches have shown that this theory can not be valid for all types of communication, due to the speed and firing rate of APs compared to the amount of information that has to be sent and processed.
It is clear that neurons in the visual system must process and transmit a huge amount of information in a short time. A experiment conducted by Thorpe, Fize and Marlot [11] showed that human visual system can process complex natural images in roughly 150 ms. A few simple equations shows that in this time just a few neurons would be able to fire APs thus their frequency would be difficult, maybe impossible to differentiate. This shows that other coding mechanisms are present in the human nervous system.

1.1.3 Human Eye & Retina

Our eye is formed by two main parts, the lens in front and the light sensing cells, called retina in the back of the eye, see figure 1.3. A similar system is used in most cameras, both analogue and digital. Light that enters the pupil, is focused and inverted by the lens, and is projected onto the retina at back of the eye. The retina consists of seven layers of alternating cells and processes which convert a light signal into a neural signal.

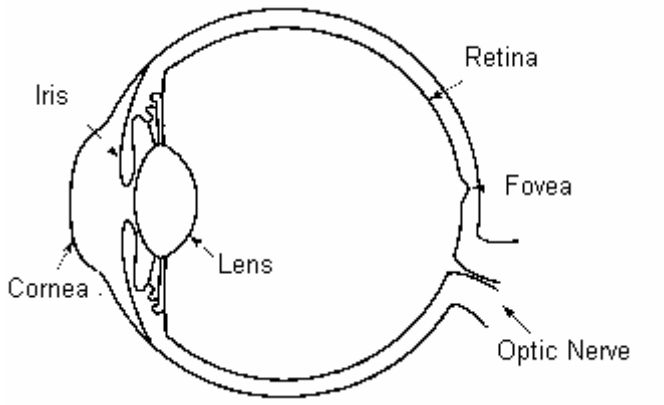

Figure 1.3

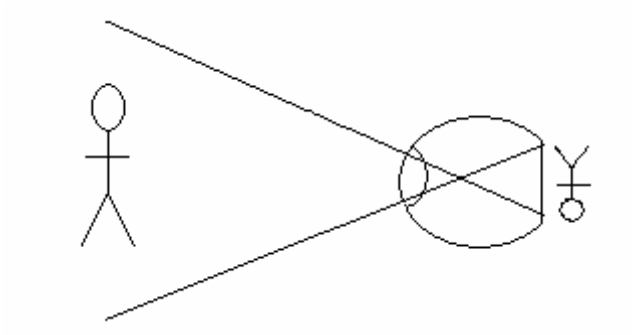

Figure 1.4

The iris is the colored part of the eye that helps regulate the amount of light that enters the eye, the cornea is the clear front window of the eye that transmits and focuses light into the eye [12]. The retina covers about 65 percent of the eyes interior surface.

Photosensitive cells called rods and cones in the retina convert incident light energy into signals that are carried to the brain by the optic nerve. In the middle of the retina is a small dimple called the fovea or fovea centralis. It is the centre of the eye's sharpest vision and the location of most color perception. With distance from the centre the resolution and the color perception decreases and the light and motion sensitivity increases [13].

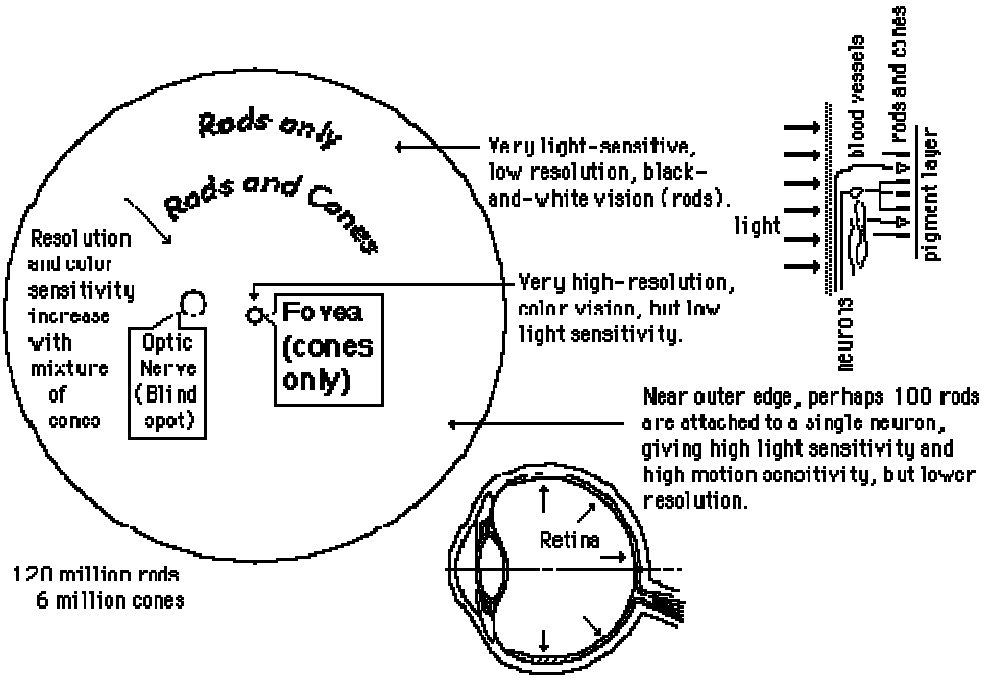

Figure 1.5

There are about 6 to 7 million cones in each eye, and they are sensitive to bright light and to color. The highest concentration of cones is in the *fovea centralis*, at the centre of the macula, containing only cones and no rods. The area in and around the fovea has a pale yellow pigmentation that is called the macula. There are 3 types of cone pigments, each most sensitive to a certain wavelength of light: short (430-440 nm), medium (535-540 nm) and long (560-565 nm). The wavelength of light perceived as brightest to the human eye is 555 nm, a greenish-yellow.
Once a cone pigment is bleached by light, it takes about 6 minutes to regenerate.

There are about 120 to 130 million rods in each eye, and they are sensitive to dim light, to movement, and to shapes. The highest concentration of rods is in the peripheral retina, decreasing in density up to the *macula*. Rods do not detect color, which is the main reason it is difficult to tell the color of an object at night or in the dark.
The rod pigment is most sensitive to the light wavelength of 500 nm. Once a rod pigment is bleached by light, it takes about 30 minutes to regenerate [14].
There are some horizontal interactions going on between the nerve cells on top of the Photoreceptors that help adapt cells to the average light level and to enhance edges.
A conceptual model that shows some of the nerve cells that lie on top of the actual photoreceptors could look something like figure 1.6.

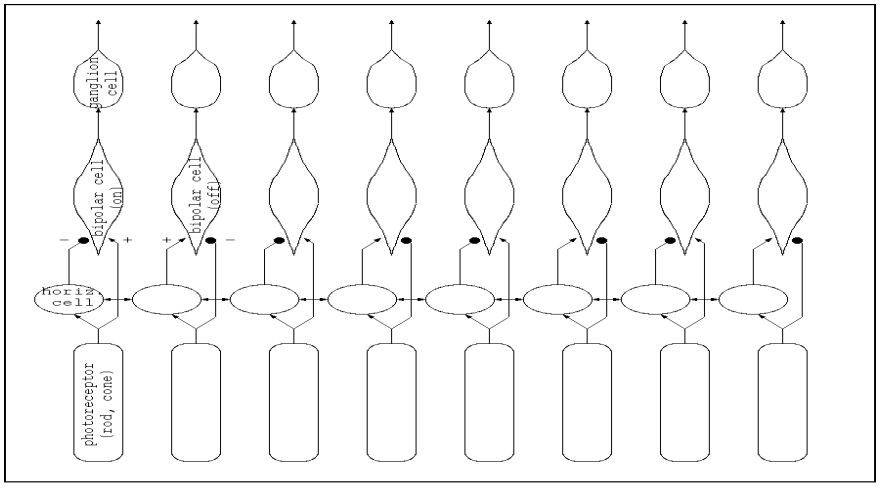

Figure 1.6

The photoreceptors are excited by light that is focused on them through the eye lens. They in turn excite so called horizontal cells that actually collect input from a group of photoreceptors and from their colleagues. Such their own activity reflects the collective average light level of a certain neighborhood. The difference between that collective light level and the local light level is computed in the bipolar cells. Some of them get excited (arrow synapses) by the direct input from the photoreceptor and subtract (bubble synapses) the collective average from it. They react to bright spots. Other Bipolar cells get inhibited by the local photoreceptor and excited by the neighborhood average. Those get excited by dark spots [15].

The cones in the eye are small and are individually connected to nerve fibers, the rods are multiply connected to nerve fibers, and a single such fiber can be activated by any one of about a hundred rods[13].
The brain actually can detect one photon of light (the smallest unit of energy) being absorbed by a photoreceptor [14].

2. A FOVEATED AER IMAGER

2.1 The eye and the digital Camera

There are many similarities in the functionality and structure between human eye and a digital video camera.
The structure of both human eye and most digital cameras, consist mainly of a lens and a sensor placed in a distance from the lens. The lens concentrates the light on the sensor and the sensor converts the light into electrical signals, see figure 1.4.
Some of the similar functionalities are that both focus on a picture, they adapt to various light levels, etc.
The main difference between them is revealed when we look at the way they process information and data. For example in the eye a lot of information processing happens locally in the actual sensor, the retina, and the result is then send to the brain for further analysis and processing but in a digital camera, the pixels are only passive components and all raw data picked by the sensors are being sent directly to a control unit for processing through an AD converter. For instance the human eye is able to find movement in surroundings, and then send the information to the brain [16], but a in motion detecting system including a camera all the data is processed in the u processor and all the calculations for finding the motion is done by the u processor.
Another big different between the eye and a digital camera, as in other digital systems is their communication system, In digital cameras, analog values picked by the pixels (light sensors) have to be send serially to an AD converter to become digitalized to binary codes and then send to the microprocessor through a parallel network.
In the human eye the information from the sensory cells are coded into electrical pulses, called action potentials (AP) in the cells and carried by the optic nerves to the brain.
In addition to these major differences; the power dissipation in a nerve system including the brain and the eye is much smaller than the power used for example in a computer and a camera that is used for motion detection.

2.2 Definition of a foveated imager

Many researchers have designed and produced different circuits and/or software that somehow imitates the functionality of the biological retina in the human eye and the result has been some intelligent silicon imagers, such as the silicon retina [17, 18]. Some of these imagers are referred to as foveated imagers based on different properties, thus different definition of a foveated imager has been presented. The definition of foveated imager used in this text is as follow: an imager with different pixel properties dependent on the distance from the centre. These properties could be size and/or computational properties.

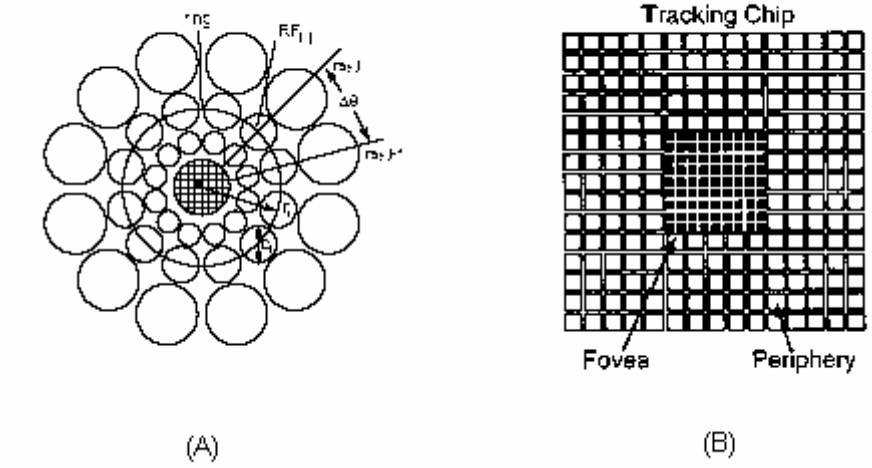

Figure 2.1

Figure 2.1 shows two examples of foveated imagers with space-variant resolution, (A) is a circuit designed by R Wodnicki [19] containing only static pixels (cons) and (B) is a tracking imager designed by Etienne-Cummings [20] containing only motion detectors (rods). In these imagers and many other [21] [22] [23] there have been used only one type of pixels with different sizes. Another type of foveated imager, like the one presented in this thesis, are imagers with the functionality and structure of the retina, with small static pixels (cones) in the centre imitating the fovea and larger dynamic motion detector (rods) in the periphery.

2.3 The pixels

The cells in the retina change their functionality from being sharp vision cells (cones) in the centre to motion detectors (rods) toward the periphery. To achieve these functionalities in the imager, we used two types of pixels that are referred to as dynamic pixels for the motion detectors and static pixels for sharp vision. Each pixel consists of a photodiode and processing circuitry. The circuitry in the static cell is mainly an integrator, it integrates a current linearly proportional to the light level over a short time, and when a threshold is reached, an AP is fired and then the pixel is reset.
The dynamic pixel fires an AP if changes in light is detected. The dynamic pixels are adaptive to various light levels and the APs are fired as the speed of that change exceeds a certain threshold.
The photodiodes in the pixels are substrate diodes made of a strong N doping in the P substrate. The static pixels are made small to produce a high resolution picture, measuring $26.8 \times 25.2 \mu m$ with a fill factor (photodiode area) of 11.3 %. The dynamic pixels are bigger, measuring $53.6 \times 50.4 \mu m$, with a fill factor of 50.4 %. The photodiode in dynamic pixels are big to achieve maximum sensitivity to light changes.
The pixel array is made up of 76×67 static cells in the centre and it is surrounded by four rows of dynamic pixels on all sides, (a total of 616 dynamic pixels). See figure 2.2.

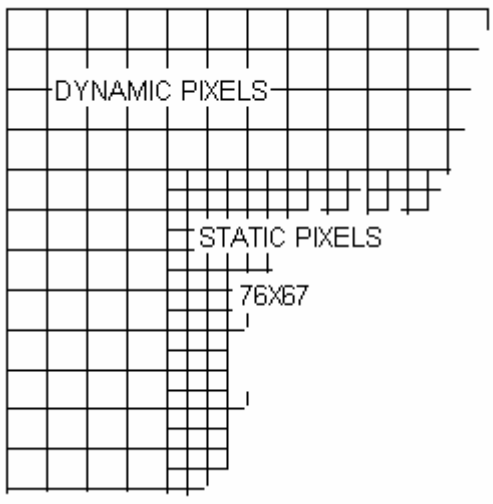

Figure 2.2

In the layout all the areas except the photodiodes are covered with a layer of metal (metal 4), this to avoid illumination of light sensitive circuits other than the photodiodes, like the transistors. To achieve good noise properties gnd guards was placed around the photodiodes.

2.3.1 The Static pixel

The static pixel can be divided in to three main parts, see block diagram below:

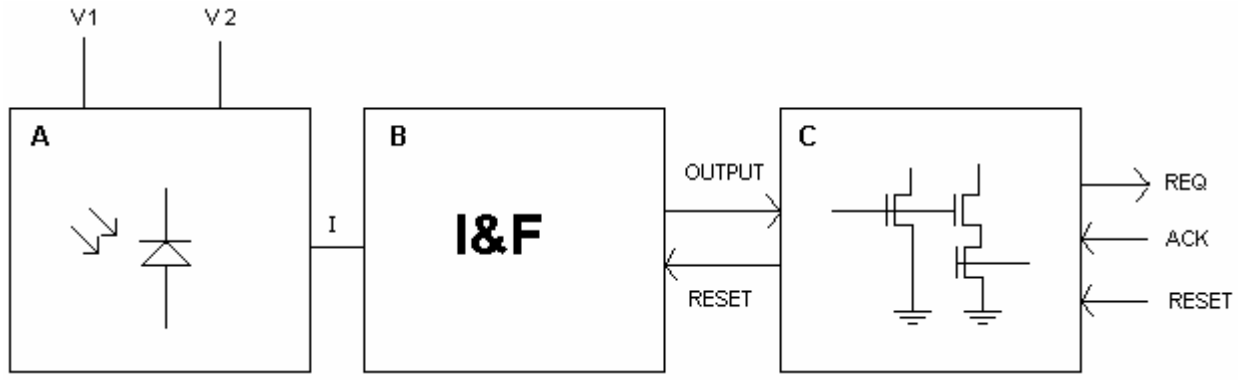

Figure 2.3

Block A is a circuit that produces a current (I) linearly proportional to the illumination of the pixel, block A contains also a current amplifier. $V1$ and $V2$ are the inputs of the amplifier, and the voltage change between them is exponentially proportional to amplification of the current amplifier.
Block B is mainly an integrate and fire circuit [2], the current from block A is integrated on a capacitor and a pulse is trigged when the potential across it reaches a threshold. The last block represents the communication with the AER that handles the communication offchip.
The static pixel will emit pulses as long a light is present, the light intensity determines the frequency.
The photo sensitive components used in the circuit are Photodiodes. Other alternatives like phototransistors were also considered, but because of the good results from earlier research [24], we preferred to use photodiode. Another reason for choosing a photodiode was the good noise properties of these components compared to the for example the phototransistor [25].

2.3.2 The dynamic pixel

The dynamic pixel can also be divided in three blocks, as shown in the figure 2.4.

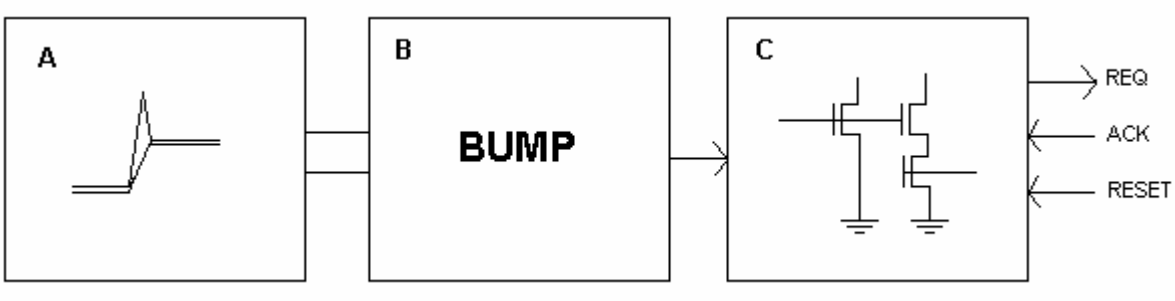

Figure 2.4

Block A handles the motion detection in the dynamic pixel. This circuit has high pass properties, adapts to the average light level and amplifies small changes in light logarithmically. Motion detected by A is sent to block B as a short voltage difference between two points in the circuit. Block B serves two purposes; 1. It rectifies the signal from the motion detector and 2. It amplifies the signal to a digital value. The digital signal from the bump circuit sets a latch in block C. The latch together with a pull down circuitry completes the communication with the AER arbiter on the periphery.

2.4 Communication

The most prominent method to approach the capacity of point-to-point connectivity in the nervous system is address event representation (AER) [26] [27]. It uses the advantage of speed in digital systems to make up for the disadvantage in density and emulates point-to-point connections by time multiplexing rather than physically implement them.
In the imager the AER protocol is used for communication with external devices. Each pixel in the imager is assigned an address by an address circuitry and the address of the pixel is sent as the information on the digital bus as that pixel produces an AP/spike. The address circuitry consists of some pull-up and pull down-transistors placed on the address line. When they are activated by an action potential they assert an address on the address-line according to their placement, the address circuitry on top assert address bits 0-7, and the one placed on the right side bits 08-15. Receivers that are supposed to receive that action potential are connected to the same bus via a decoder and get stimulated when their address occurs. The bus can only transmit APs serially but it can do it much faster than an axon. It can transmit APs so tightly spaced in time [28] that for a network of neurons that operate on a natural timescale these pulses are virtually simultaneous.
All the pixels in the camera are placed in rows and columns with horizontal and vertical address lines connecting them to the AER arbiter and the address circuitry placed on top and the right side of the pixel array. The dynamic pixels are twice as large as the static pixels, thus every second address line from static pixels connects to them. The output of each pixel is connected to a circuit (see chapter 3.8) that communicates with the AER arbiters on the periphery of the pixel array. The AER arbiter at the top of the pixel array will be referred to as X-ARBITER and the one at the right as the Y-ARBITER, see figure 2.5.

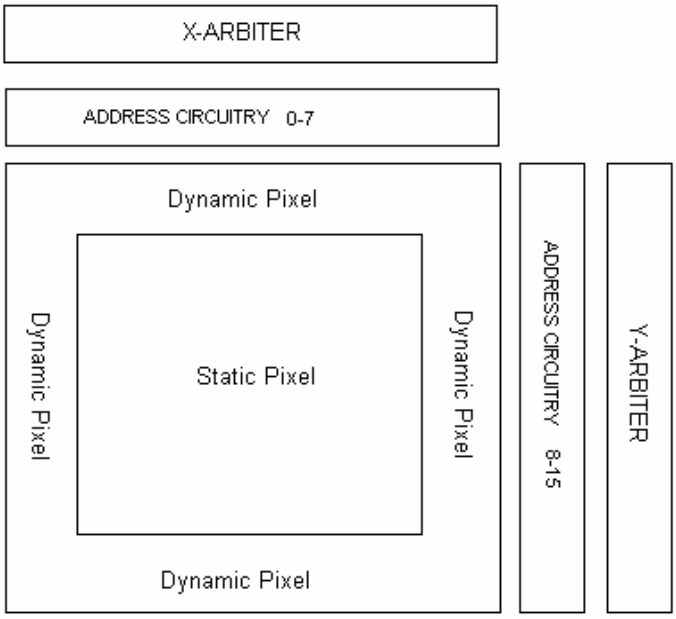

Figure 2.5

Figure 2.5 Shows the structure of the imager, with static pixels in he centre, surrounded by the motion detectors (Dynamic pixels). On the top and right side of the pixels-array there are first the two address circuitry that assigns each pixel a binary address and then the X and Y arbiters.

2.5 The imager

Figure 2.6 shows a picture taken by the imager. A Software is used to show the result of the imager on the computer screen.
The software integrates pulses from the static pixels from the same address in a time period and draws a square with a color proportional to the amount of spikes in the same address as the pixel on the screen. White pulses are the maximum amount of pulses and the black is 0 pulses and other pixel values get a grayscale dependent on the amount of the pulses generated by the pixel in the imager. The quality of the picture is increased if the integration time increases, but the frame rate will decrease.
The dynamic pixels will whiten a pixel fully if they detect a motion once and fade thereafter.

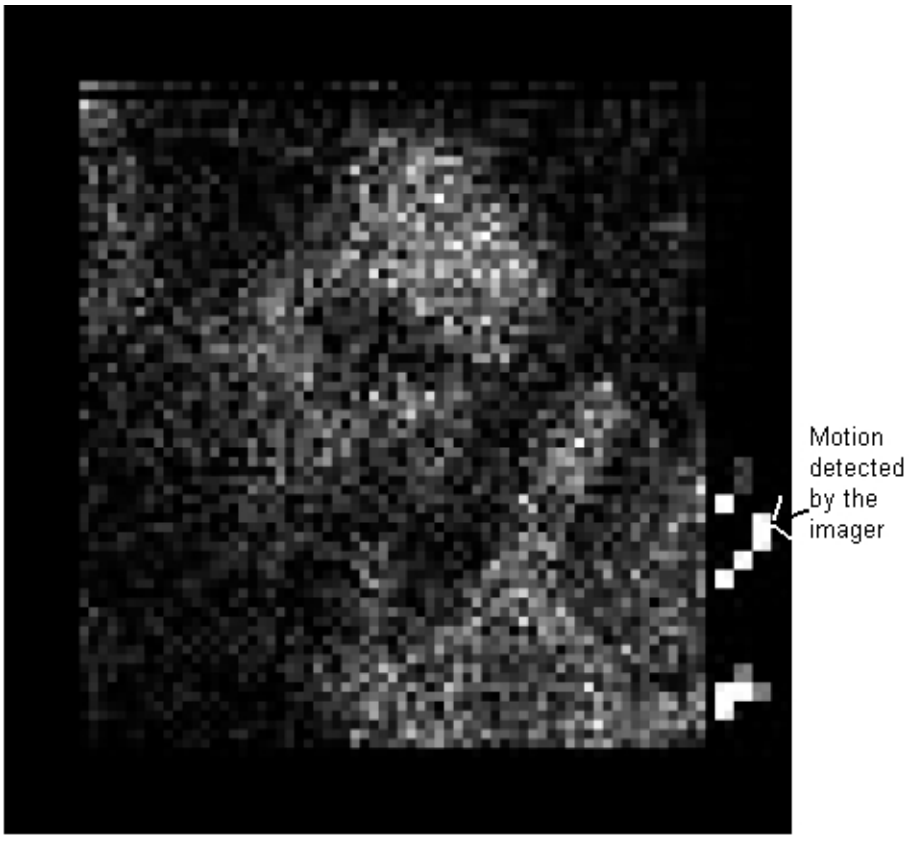

Figure 2.6

In figure 2.6 we see a person waving his hand in the centre of the picture and the motion is detected in the periphery as big white squares.
The static pixels in the centre suffer from salt and pepper noise due to the mismatching between the transistors. This salt and pepper noise is observed on the picture as non uniform drawing of pixels in places where two pixels receive the same amount of light. The mismatching in the static pixel is discussed in detail in chapter 3.3 and is shown in a MonteCarlo simulation in appendix C, figure C.7. In figure C.7 we see a variation in the amount of spikes produced by the static pixels from 300 KHz to 1MHz.

3. IMPLEMENTATION

In this chapter all the circuits used in the imager are discussed and the test results are shown. The schematic of all circuits are also shown and reasons for choosing the different solutions are presented. The layout of a complete dynamic pixels and static pixel is presented in this chapter and other layouts are presented in appendix D.

3.1 Test Setup

All the measurements with light were done in a dark room with a red colored LED placed 10 cm from the pixels without the lens. The LED was connected to a function generator in series with a resistance. See figure 3.1.

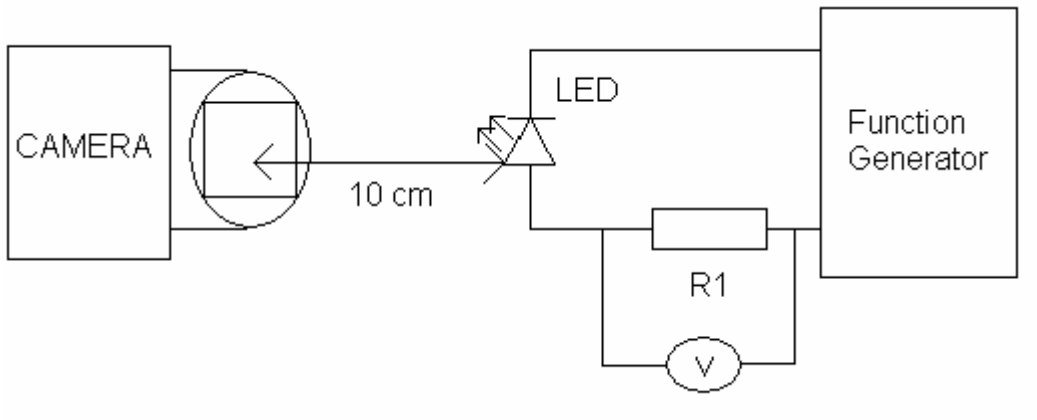

Figure 3.1

The light intensity of the LED is linearly proportional to the current through the LED and the series connected resistance R1. By measuring the voltage across R1 and divide that by R1, the current through the LED was calculated.
The LED used in the test has a threshold voltage of approximately 0.8 V and the series resistance is 270Ω. The LED's light intensity was measured with a LUX*meter placed also10 cm from the LED for various current values through the LED and a relation between the current and light intensity was obtained, see figure 3.2.

*Lux here is the measure for irradiation, corrected for the wavelength spectrum of human vision. 1 Lux of red light of $650\eta m$ wave length corresponds to an irradiance of 0.015 Watts per square meter

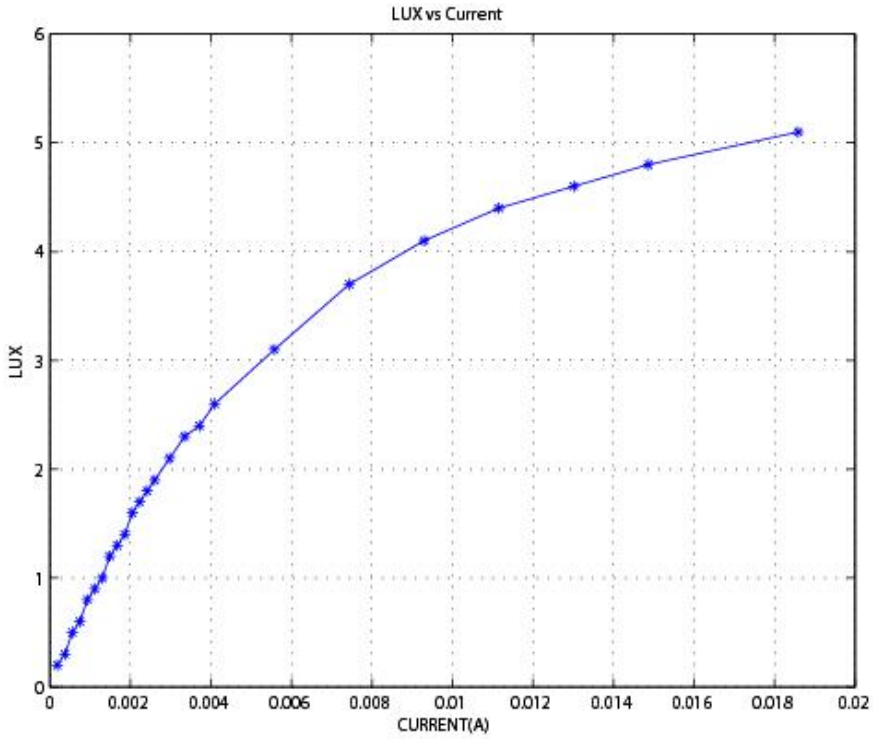

Figure 3.2

From the figure we see that the LED has a linear increase in light intensity in the beginning and it flats out and decreases for larger values. This misbehavior is caused by saturation because of the LED properties.

All the circuits used in the imager were also implemented as a separate test circuits outside the imager on the same chip, this to have access to all the circuits separately and at the same time achieve the same operating condition (temperature, light) as the circuits in the imager.
There were conducted two types of tests on the imager, a test directed at the static pixels and another test at the dynamic pixels. When testing the static pixels, the dynamic pixels were shut off and vice versa to isolate the test objects.
Two properties of the static pixels were measured, 1. the response of the current mirror in the static pixel and 2. the response of the whole pixel array of static pixels.
The dynamic pixel was tested in more detailed as more complicated circuits were used. We tested the motion detector without and with the bump circuit. In addiotion, in the appendix C we have presented some of the simulation results for the dynamic and static pixels.

V1	3.19
V2	3.3
VPHOTO	1.2
VBUMP	0.42
VLEAK	0.2
VOPAMP	0.7
VREF	1.2

Table 1: *Parameters used for the measurements presented in the thesis, unless stated explicitly.*

3.2 The photodiode

When the reverse biased PN-junction is illuminated, see figure 3.3, the photons impacting the junction causes covalent bonds to break, and thus electron-hole pairs are generated in the depletion layer. The electric field in the depletion region then sweeps the librated electrons to the n side and the holes to the p side, giving rise to a reverse current across the junction. This current is proportional to the light intensity [29].

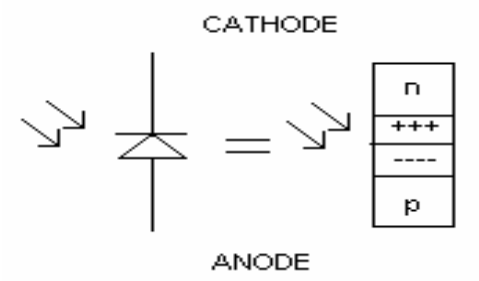

Figure 3.3
Other than the light properties, the photodiode acts as a normal diode.

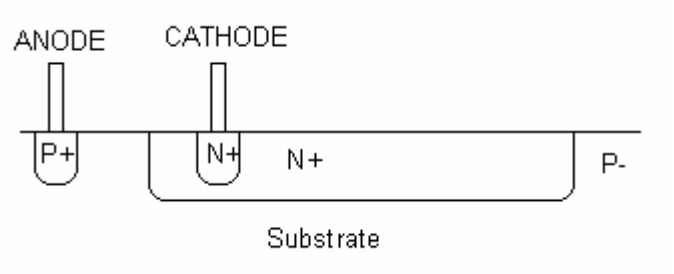

Figure 3.4

An extremely small current exists in the reveres bias when diode is not illuminated. This current is caused by minority carriers in the n and p region that are produced by thermally generated electron-hole pairs. This current is referred to as dark current for photodiodes.

3.3 Current amplifier

The exact amount of current generated by the photodiodes used in the circuit was unknown, and a circuit that made us able to regulate that current was necessary. The problem was solved by using a tilted current mirror.

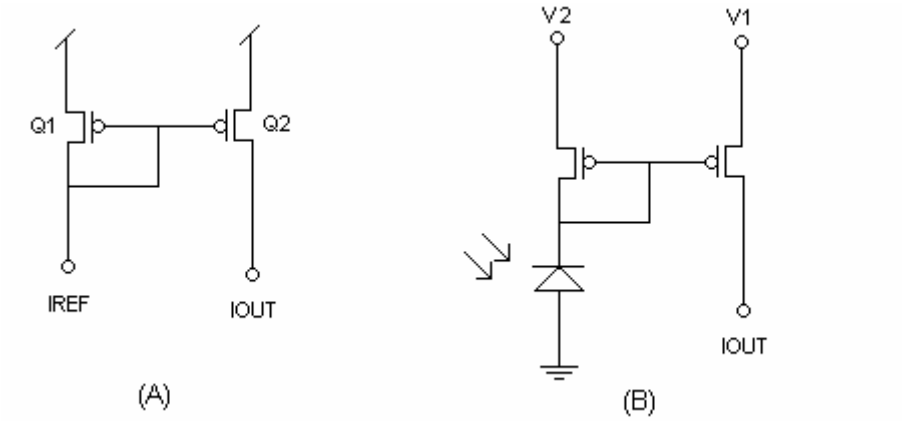

Figure 3.5

A simple current mirror also referred to as Constant-current source is shown in figure 3.5 A. The heart of the circuit is transistor $Q1$, whose gate is shorted to its drain, and thus is operating in the saturation region. To achieve the same functionality on $Q2$ as $Q1$ (to keep $Q2$ in saturation), its drain voltage is limited to:

$$V_{D2} < V_{DD} - V_{SG2} + |V_{TP}| \qquad \text{Equation 3.1}$$

The current through each branch is given by:

$$I_{REF} = Is \exp\left(\frac{V_G - V_{T0} - nV_1}{nU_T}\right) \qquad \text{Equation 3.2}$$

And

$$I_{OUT} = Is \exp\left(\frac{V_G - V_{T0} - nV_2}{nU_T}\right) \qquad \text{Equation 3.3}$$

Where

$Is = 2n\beta U_T^2$ And

$\beta = \frac{W}{L}\mu C_{ox}$ W is the width and L is the length

We have:

$$(W/L)_1 = (W/L)_2$$

Equation 3.2 and 3.3 describe the behavior of a NMOS, but by changing the sign and neglecting the effects of slope factor, we can deduce the amplification as:

$$\frac{I_{OUT}}{I_{REF}} = e^{\frac{V_2 - V_1}{U_T}} \qquad \text{Equation 3.4}$$

From equation 3.4 we see that the relation between I_{OUT} and I_{REF} is exponentially related to the value of the drain voltages on V_1 and V_2. By changing the voltage at each branch separately, $V1$ and $V2$, see figure 3.5 B, we can achieve amplification or attenuation of the current.

Component sizes of the Current mirror and D1.

Component	Width	Length
Q1	**2.5**	**1.4**
Q2	**2.5**	**1.4**
D1	**12**	**6.5**

Table 2

THE RESPONCE

Figure 3.6 shows the results from tests on the current mirror together with the photodiode. As mentioned earlier a red colored led was placed 10 cm from camera and the camera was illuminated with different light levels according to the graph on figure 3.2. $V1$ was kept constant at 3.3 volts and the voltages on $V2$ are showed on the graph. The X axis is the light intensity in lux and the Y axis is the current produced by the current mirror. The average current was measured by reading the average voltage across a 1 MΩ resistance in series with the output of the current mirror. The blue line shows the result for $V2$ at 3.16 volts and the red line at 3.19 volts. At 0 lux we can se a current due to the dark current. This current is one of the reasons for the so called salt and pepper noise in the picture, this is shown in chapter 2.5, figure 2.6.

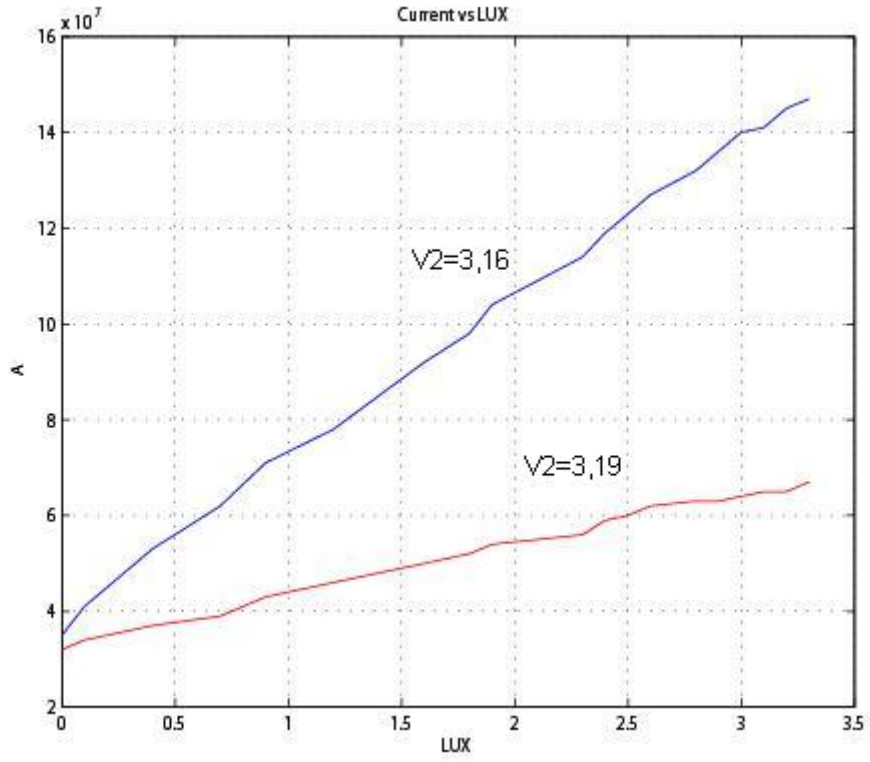

Figure 3.6

The size of the photodiode used in this test, is 25x37 um and the transistors in the current mirror are 2.5 um wide and 1.4 um long.

3.4 I&F Circuit

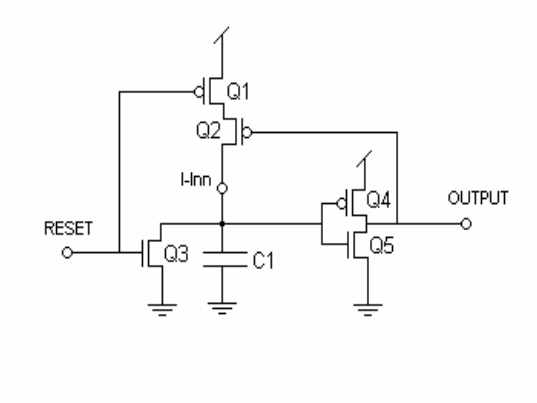

Figure 3.7

Figure 3.7 shows the integrate and fire (I&F) circuit used in the imager, a good example of a mix-mode circuit. The output of the current mirror (IOUT) is connected to I-INN. The current produced by the current mirror (see page 26) charges the capacitor $C1$, and when the voltage across it reaches the threshold of the inverter, the inverters output changes state from 1 to 0, (digital values). Through a feedback $Q2$ is activated and $C1$ is stabilized at vdd, this is only possible if the reset signal is low. When the reset is asserted, $Q1$ will deactivate and separate C1 from vdd and at the same time $Q3$ empties the charges on $C1$ to gnd, and the initial state is reached. The size of $C1$ is essential for how fast the threshold voltage of the inverter is reached.

The current through a capacitor can be expressed by the voltage change of the voltage across it:

$$i = C\frac{dv}{dt} \qquad \text{Equation 3.5}$$

Expression for the voltage as a function of the current is:

$$v(t) = \frac{1}{C}\int_0^t id\tau + v(0) \qquad \text{Equation 3.6}$$

having $v(0) = 0$

$$v(t) = \frac{1}{C}\int_0^t id\tau \qquad \text{Equation 3.7}$$

From equation 3.7 we see that small capacitor makes the circuit noisy due to the dark current, it reaches the threshold faster (the dark current becomes more effective), on the other hand a big capacitor is more immune to the dark current (it needs bigger current values to reach the threshold) and the circuit becomes slower. The area of the capacitor in the I&F circuit measures 2.4752e-4 um and has a value of 221.576f F.

Component sizes of the I&F.

Component	Width	Length	Value
Q1	**0.8**	**0.55**	
Q2	**0.8**	**0.55**	
Q3	**0.8**	**0.55**	
Q4	**0.9**	**0.35**	
Q5	**0.5**	**0.35**	
C1			221.576f F

Table 3

The response of the static pixels in the imager is measured as the average pulse in a time period (0.1secounds) versus light intensity of the whole pixel array of static pixels.

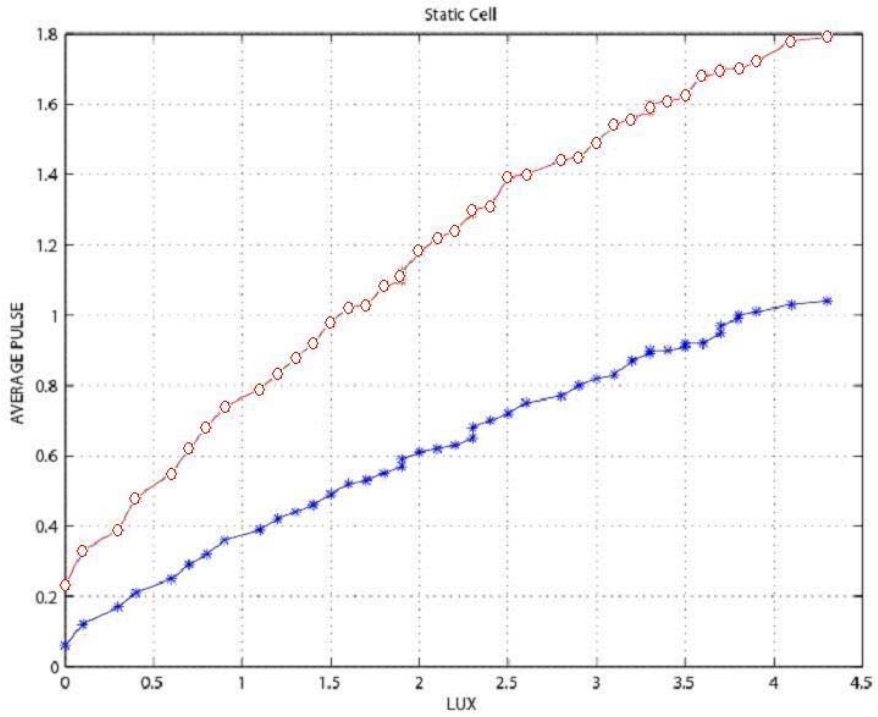

Figure 3.8

Figure 3.8 shows the result from the test on the static pixels in the camera, The X coordinate is light intensity in lux and the Y coordinate is the average pulses of all the pixels in the imager in a time period. In this test $V1$ is 3.3 volts. The red graph (circles) is the result with $V2$ at 3.16 and the blue graph (stars) $V2$ at 3.19 volts. We see that both graphs grow linearly with different slopes (amplification). At 0 lux we would expect 0 pulses for both graphs, but due to the mismatch between transistors there are pulses produced by the pixels. These pulses are considered as an offset compared to complete dark. We see that the offset in the circuit is larger for small values of $V2$ (bigger amplification).

Figure 3.9 shows the complete layout of the static pixel. More than half of the area of the circuit is the capacitor $C1$ that gathers charges from the photodiode.

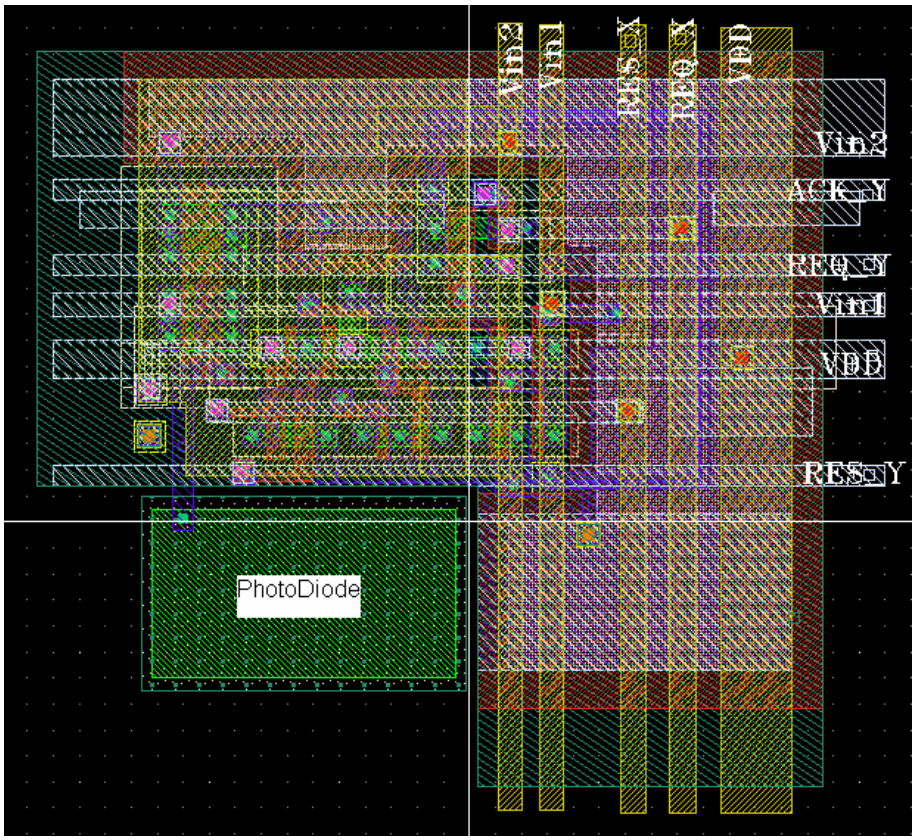

Figure 3.9

The connection lines REQ_X, REQ_Y, ACK_Y, RES_X and RES_Y and VDD are crossing the the static cell to achieve connection to the arbiters on the periphery and power suplies. The cell, except the photo diode is coverd by metal 4 layer to aviod illumination of the light sensitive components in circuit. Metal 4 layer is connected to gnd.

3.5 Motion detector

The motion detector used in the dynamic pixels is based a circuit designed by Delbrück et al. [30].

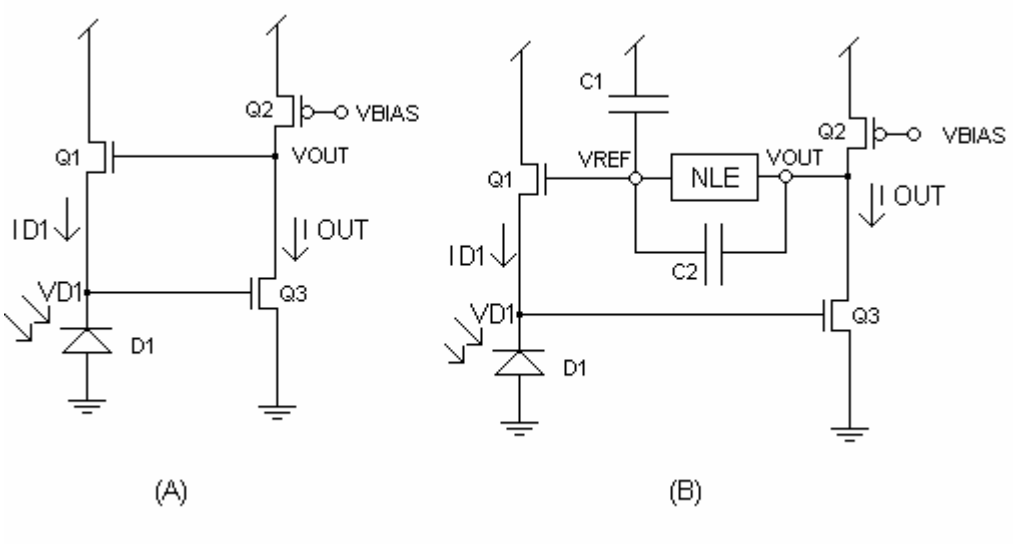

Figure 3.10

The circuit is basically an amplifier with a negative feedback. To understand the circuit, we can first look at the simplified version in figure 3.10(A). Illumination of $D1$ will cause the current $ID1$ to increase and the voltage $VD1$ to drop. The voltage change in $VD1$ is then inverted to VOUT. The increase in VOUT increases the current through $Q1$ and raises $VD1$ to its initial value. The high gain in the feedback loop clamps $VD1$, there will be a small voltage change in $VD1$ compared to the initial value, but its negliable. By changing the bias on $Q2$, we are able to influence the value of VOUT.

The equations below describe the behavior of the circuit in figure 3.10(A).

$$I_{D1} = I_s e^{\left(\frac{V_G - VT_0 - nVS}{nUT}\right)} \qquad \text{EQUATION 3.8}$$

Equation3.9 is the formula for a transistor operating in subthreshold.

Assuming: $n = 1$.

$$I_{D1} = I_s e^{-\left(\frac{VT_0}{UT}\right)} e^{\frac{1}{UT}(VOUT - VS)} \qquad \text{EQUATION 3.9}$$

Having: $I_s e^{-\left(\frac{VT_0}{UT}\right)} = I_0$, $\frac{1}{U_T} = C$, $V_G = VOUT$ and $V_S = VD1$

$$\lg I_{D1} = \lg I_0 + C(VOUT - VS) \qquad \text{EQUATION 3.10}$$

$$\lg I_{D1} = \lg I_0 + CVOUT - CV_{D1} \qquad \text{EQUATION 3.11}$$

$$VOUT = \frac{\lg I_{D1} - \lg I_0 + CV_{D1}}{C} \qquad \text{EQUATION 3.12}$$

$$VOUT = \frac{\lg I_{D1}}{C} - \frac{\lg I_0}{C} + V_{D1} \qquad \text{EQUATION 3.13}$$

Equation 3.13 shows that the VOUT is logarithmically dependent on the current through the Photodiode, I_{D1}, large negative feedback. From equation 3.13 w can also see that VOUT is linearly proportional to the voltage across the photodiode V_{D1}.

In figure 3.10 (B) the feedback lines is replaced by capacitive voltage divider, $C1$ and $C2$ and a NLE (Non Linear Element). A NLE, also called adaptive element is shown in figure 3.13(A) and its V/I behavior is shown in figure 3.13(B). The NLE behaves like a mos diode and a bipolar diode in parallel, with opposite polarity.
The current increases exponentially with voltage for either sign, and there is an extremely high-resistance region around the origin, as shown in Figure 3.11 (B). This behavior makes the circuit sensitive for small changes and gives it fast adaptation for large changes in light. In the motion detector, when VOUT is larger than VREF, the NLE acts as a CMOS diode, and when VREF is larger than VOUT it becomes a bipolar diode.

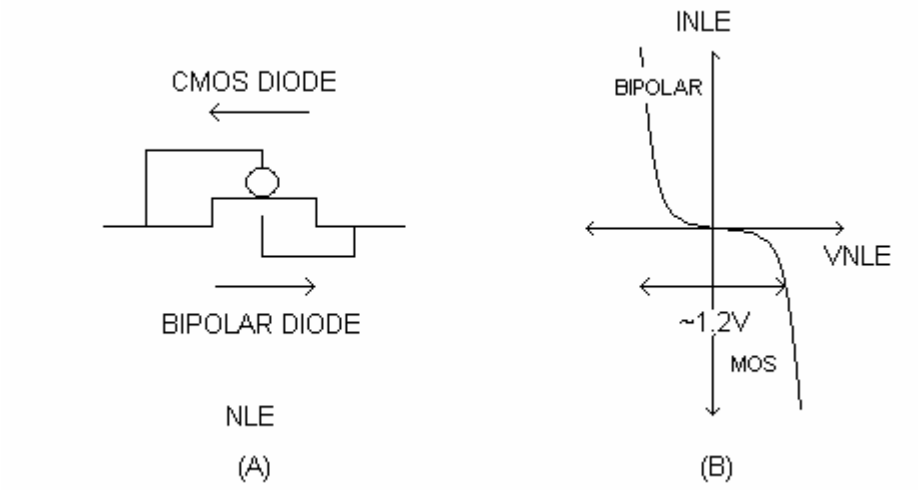

Figure 3.11

The capacitor $C1$ serves two purposes: 1, together with $C2$ it acts as a voltage divider to limit the negative feedback 2, together with NLE it acts as a kind of a memory to store an analog value on the floating point VREF. A good description of VREF is given by Delbrück, calling VREF a predicted value that is adjusted continuously when compared to the input by $Q1$.
If the voltage change in VOUT is slow (DC behavior), the NLE will allow charges into or from $C1$, depending on the light change direction, and adjust VREF.

When the voltage change in VOUT is fast and small (AC), $C2$ and $C1$ will act as a voltage divider and give VREF a value depending on the relation between $C1$ and $C2$ according to:

$$\Delta VREF = \Delta VOUT \frac{C1}{C1 + C2} \qquad \text{Equation 3.14}$$

Figure 3.13 shows the test result from the motion detector. In this test we had a blinking LED in front of the cell. In this figure we see clearly that the circuit works by studying the response of the VOUT and VREF. First we see that VOUT increases instantly due to an increase in light intensity and almost simultaneously VREF follows to adapt to the new conditions. The increase in VREF is smaller than the VOUT because of the affect of the capacitor feedback (Equation 3.8). After VOUT reaches a peak it decreases toward VREF till they get the same value. By taking a closer look at the graph we see that also VREF decreases and follows the same pattern as VOUT, but this change is much smaller than the change in VOUT. The circuit's reaction to light changes is not symmetric, the reaction from light to dark is weaker than from dark to light. This non symmetric behavior is caused by the non symmetrical properties of the diodes in the NLE. The actual behavior of the NLE is shown in figure 3.12(B) and the ideal behavior is 3.11 (B). In figure 3.12 (B) we can see that the threshold of the bipolar diode is smaller than the MOS diode.

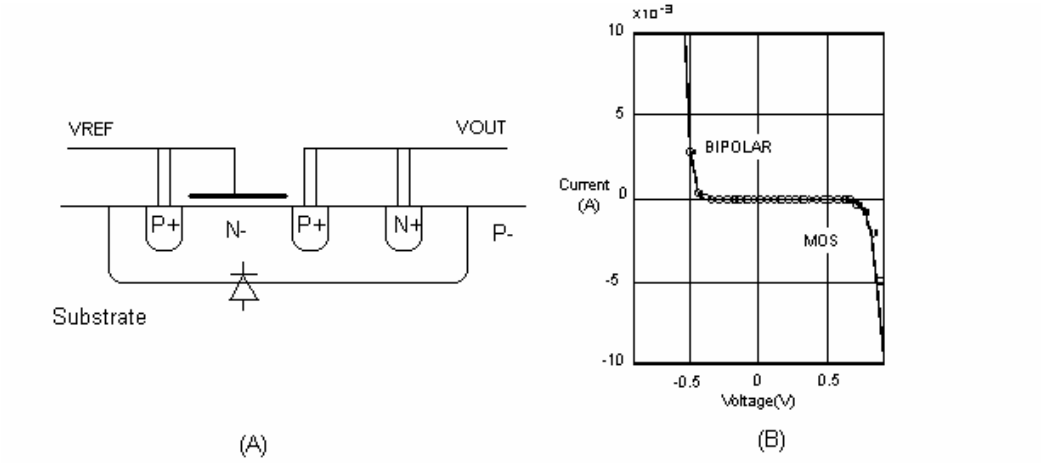

Figure 3.12

Component sizes of the motion detector.

Component	Width	Length	Value
Q1	2.5	1.4	
Q2	2.5	1.4	
Q3	2.5	1.4	
C1			147.898f F
C2			18.676 f F
D1	48	30	
NLE	1	2	

Table 4

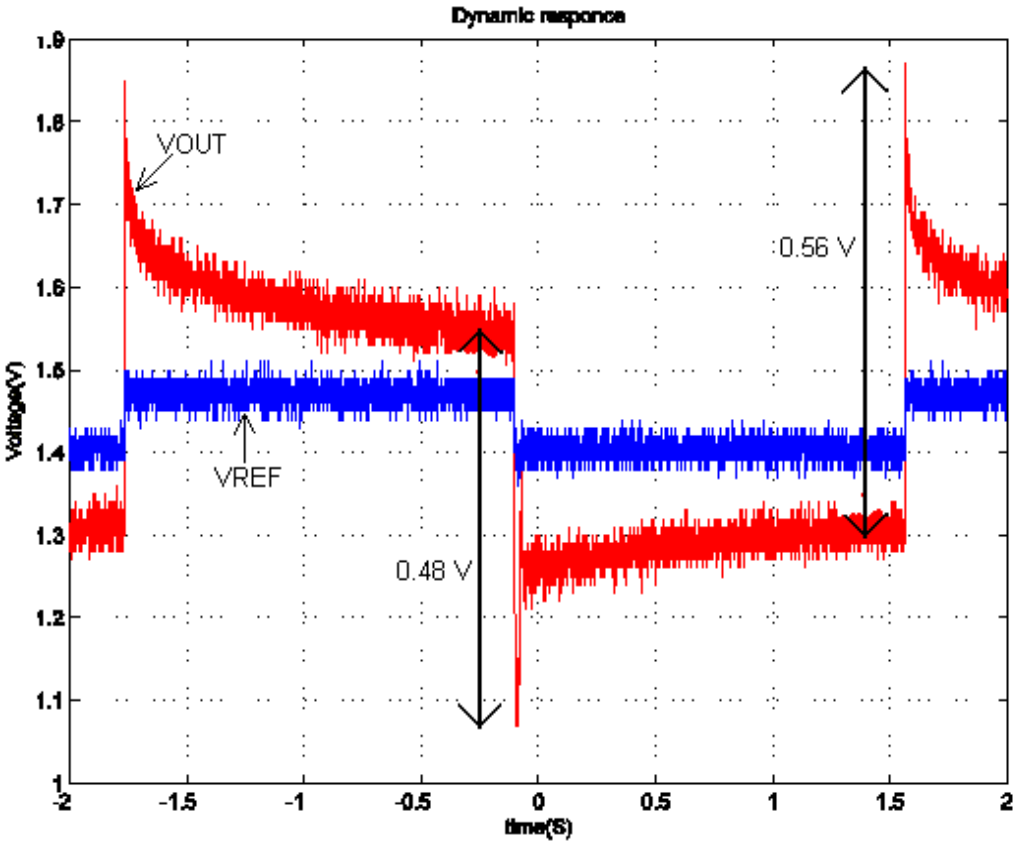

Figure 3.13

When the NLE acts as a bipolar diode, it is also affected by a leakage to ground. This leakage is caused by the PN junction created between the N well and the substrate, see figure 3.12 (A). In our circuit this leakage is ignored because VOUT is driven actively and the leakage is compensated, but if the NLE is connected opposite way, the leakage will become more noticeable by causing a voltage difference between VREF and VOUT.

3.6 Other properties

Beside the unsymmetrical behavior of the circuit, the circuit reacts as expected to light changes if there is a background illumination. But when the light change is from light to completely dark, another phenomenon is observed.
VOUT reacts much more powerful than it is supposed to on its way down, and then it returns to its final destination by an opposite jump, see figure 3.14, the undesirable jump is marked with an arrow.
The following graphs on the next five pages confirm this measurement. In these tests, the LED used to test the circuit was fed with digital pulses. I started my test with having the LED switch from strong illumination to completely dark to strong illumination to weak illumination (having a light present all the time). This transition was done in five steps by increasing the lower value of the voltage pulse on the LED.
The LED started to illuminate when the voltage across it become larger than 0.8 volts. By choosing the offset on the function generator to 2.5 V and change the amplitude according to table 1 we achieved the various test results. The bias voltage on the motion detector was 1.2 V.

	FIG 3.14	FIG 3.15	FIG 3.16	FIG 3.17	FIG 3.18
Offset	2.5V	2.5V	2.5V	2.5V	2.5V
Amplitude	3.4V	3.3V	3.2V	3.1V	3.0V
V MAX	4.2V	4.15V	4.1V	4.05V	4V
V MIN	0.8V	0.85V	0.9V	0.95V	1V

Table 5

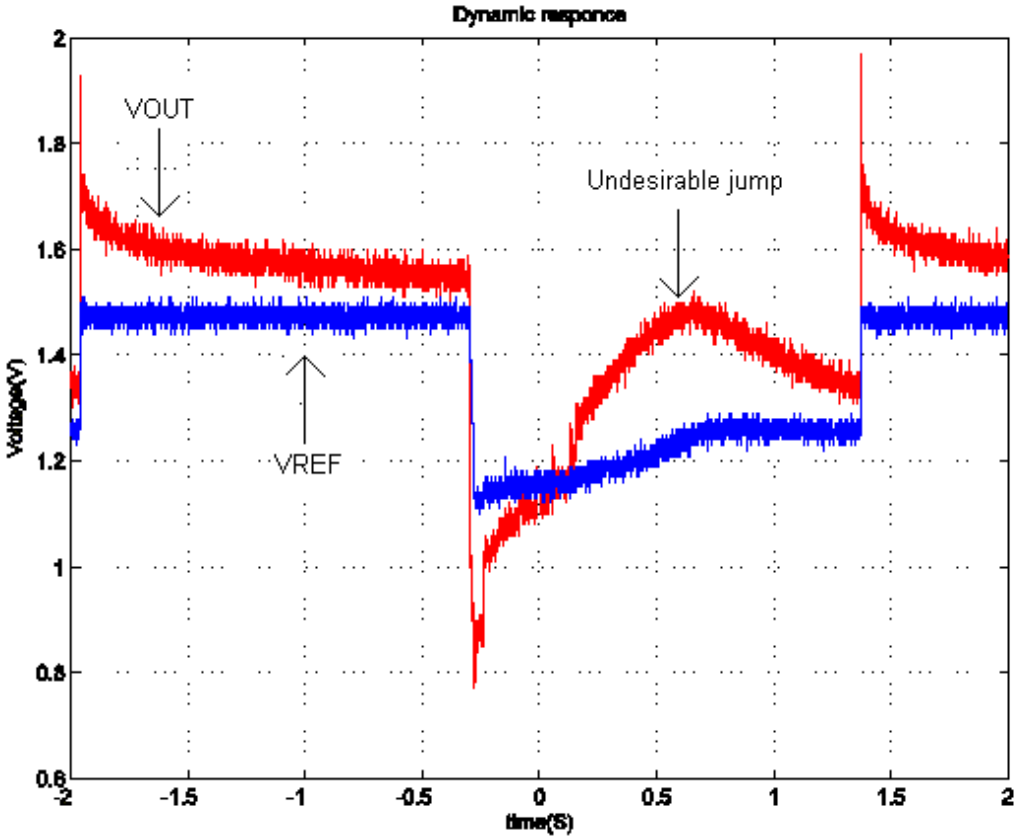

Figure 3.14

Figure 3.14 shows the result from the first test, from strong illumination to completely dark, VMIN was at 0.8 volts (see table 5). On this figure we clearly see the strange behavior of the circuit. The positive jump, transition from dark to light, is as expected, but the negative transition is followed by a jump with the opposite polarity.

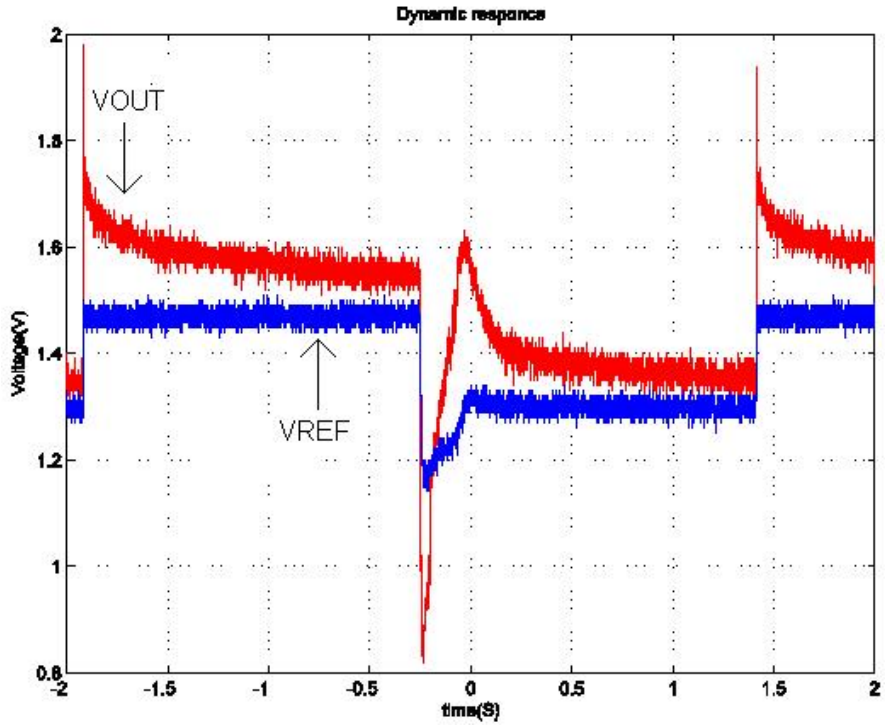

Figure 3.15

The undesirable jump moves toward the starting point and becomes sharper. Also the amplitude of the down pulse is decreased by ca 0.1 volts to 0.75 volts. Here VMIN is 0.85 mV, giving a weak Illumination (see table5).

,

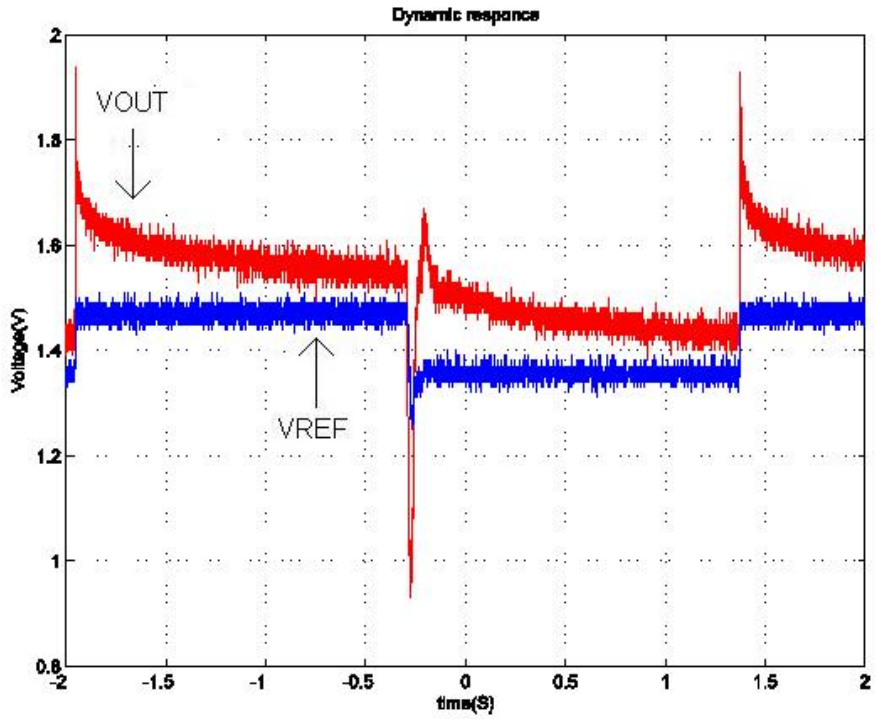

Figure 3.16

Again we can see that the undesirable jump moves toward the starting point and becomes even sharper. Also the amplitude of the down pulse is decreased by ca 0.1 volts to 0.6 volts. VMIN in this test is 0.90 volts (see table 5).

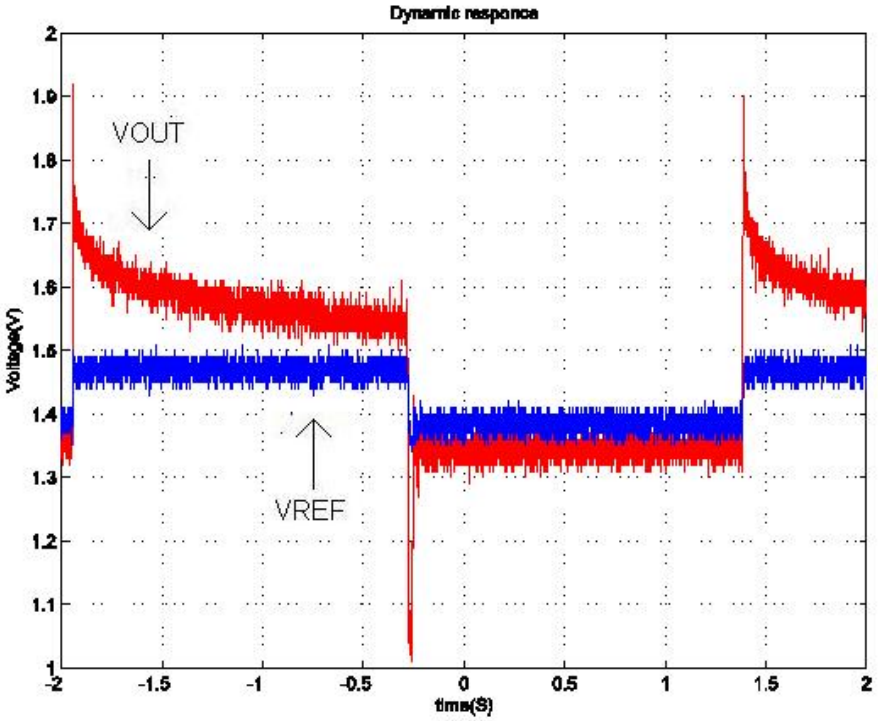

Figure 3.17

In this graph we can see that the undesirable jump almost disappears and the down going pulse is very sharp. The amplitude of the down pulse is decreased by ca 0.1 volts to ca 0.55 volts. Here we have a light present all the time, even though the illumination is very weak, VMIN is 0.95 V in this test (see table 5).

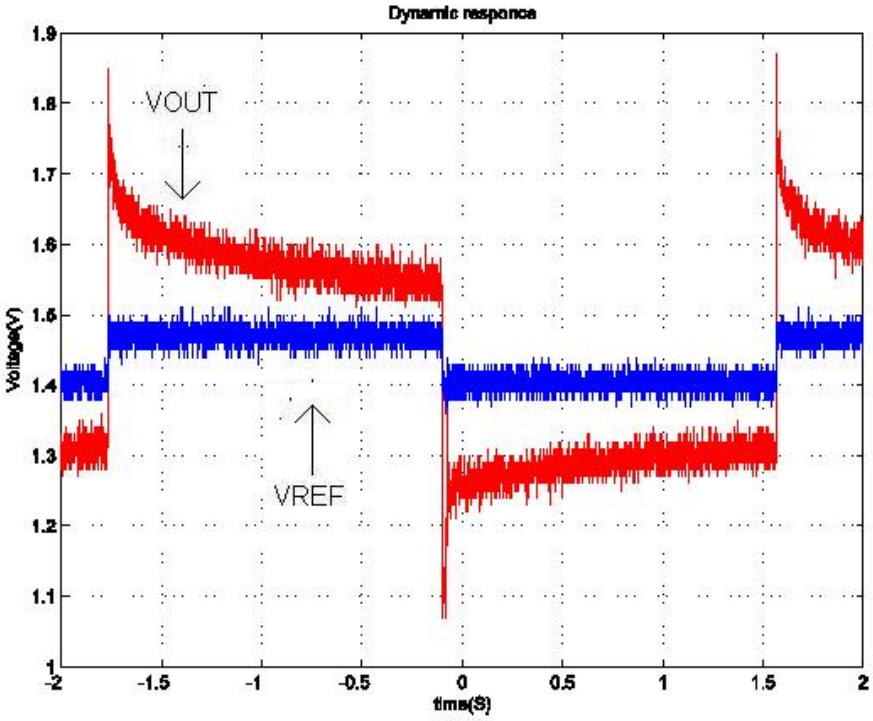

Figure 3.18

In this figure the undesirable jump has almost vanished as the weakest light level is stronger, except the unsymmetrical behavior discussed earlier, the circuit acts as expected. In this test an illumination was present all the time. VMIN is 1V in this test (see table 5).

The reason for the undesirable jumps shown in figures 3.14, 3.15, 3.16 is basically the delay in the circuit. When the photodiode is illuminated, there is a stable voltage at $VD1$ and a strong current will follow through $D1$. When the illumination stops, the current through $VD1$ decreases exponentially and its reaction becomes slow and the delay in the feedback line increases. This is sown as a block diagram in figure 3.19. In this figure the input (inn) represents the photodiode and the output (out) VOUT.

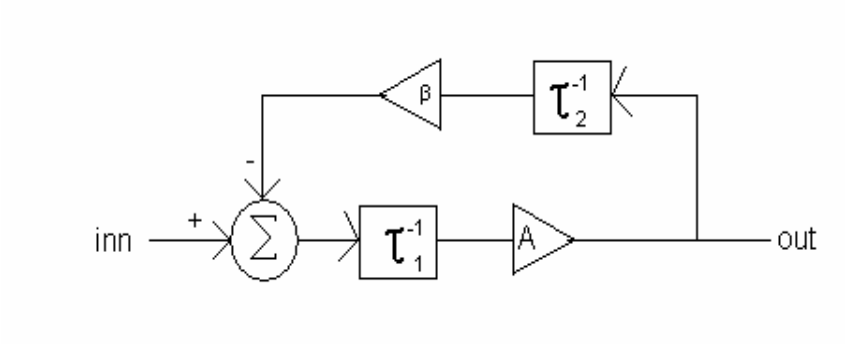

Figure 3.19

τ_1^{-1} represents the delay in the feedforward and τ_2^{-1} is the delay in feedback line.
When VD1 rises due to the light decrease, $Q3$ pulls VOUT low. How low VOUT goes depends on the bias voltage on the $Q2$. From figure 3.14 we see that the VOUT drops from ca 1.55 to ca 0.78 volts, and VREF drops from ca 1.45 to ca 1.12 volts. The voltage drop on VREF weakens $Q1$ and $Q3$ and thus VOUT is pulled up by $Q2$, and again VREF follows. These ups and downs on VOUT continue until a stable operating point is reached, VOUT will oscillate to its final value.
This problem can be reduced by increasing the bias voltage on $Q2$. Increasing the bias voltage increases the delay in the feedforward line and a matching between the forward delay and the delay in the feedback line is established. In the figures 3.21, 3.22, 3.23 on the next pages we have shown 3 test results with different bias voltages.

Figure	Bias voltage
3.21	0.7 V
3.22	1.7
3.23	2.2 V

Table 6

From the graphs we can see that by increasing the bias voltage this problem almost disappears. As the bias voltage increases, the current through $Q2$ gets weaker and the feedforward becomes slower, thus a better matching between the delay in the feedback line τ_2^{-1} and the forward line τ_1^{-1}. This can be observed in figure 3.23.
In figure 3.22 the oscillation of VOUT is clearly shown.

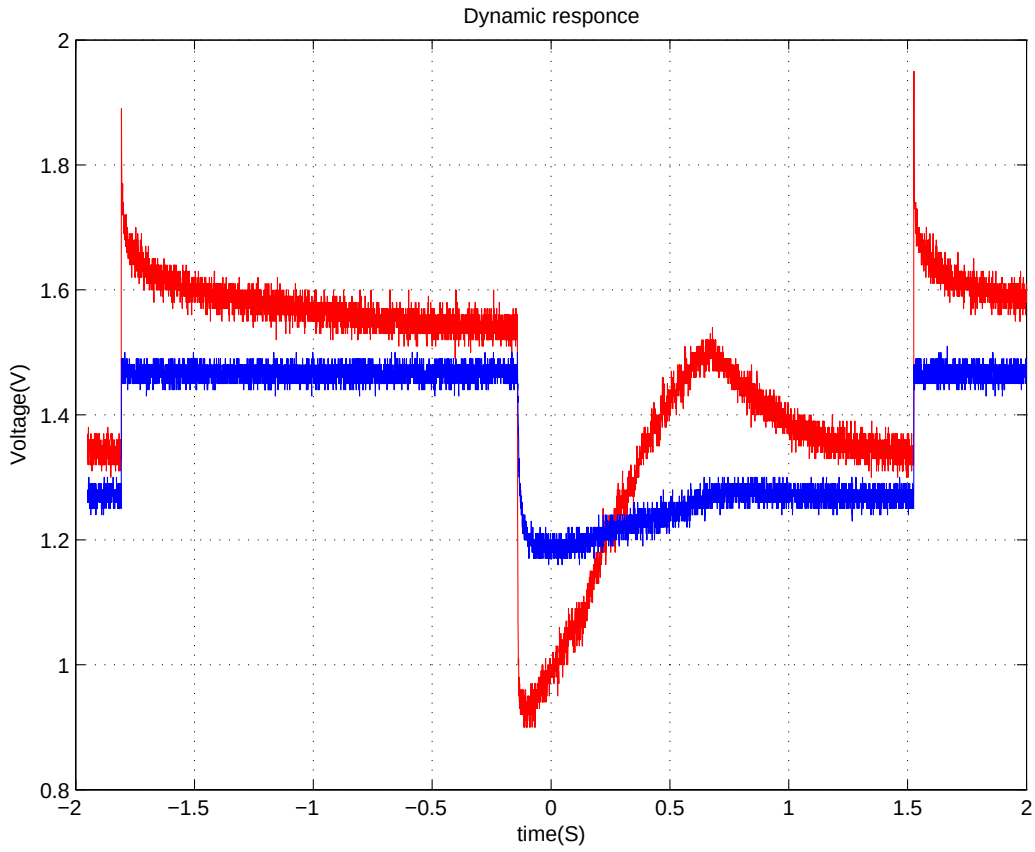

Figure 3.21

This figure shows the test result with a bias of 0.7 volts. We can see that the undesirable jump is clearly shown. This jump can be translated as a signal by the rest in the pixel and produce a false AP.

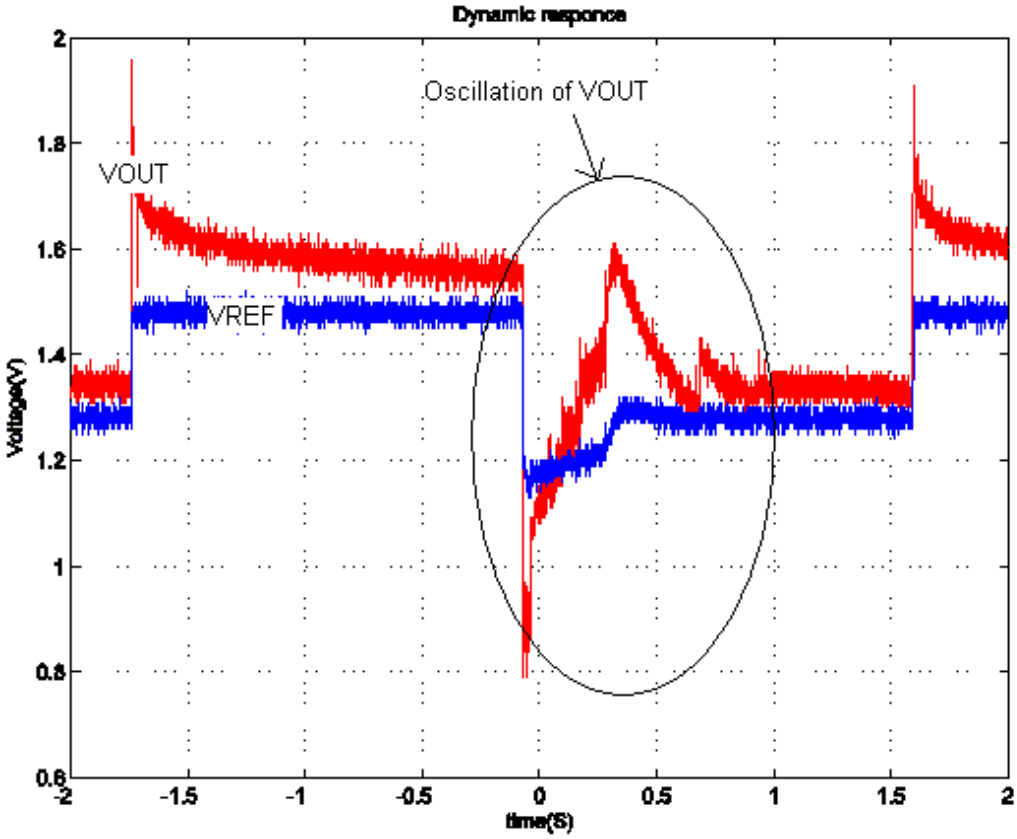

Figure 3.22

This figure shows the test result with a bias of 1.7 volts. With this bias voltage the oscillation of VOUT is clearly observed.

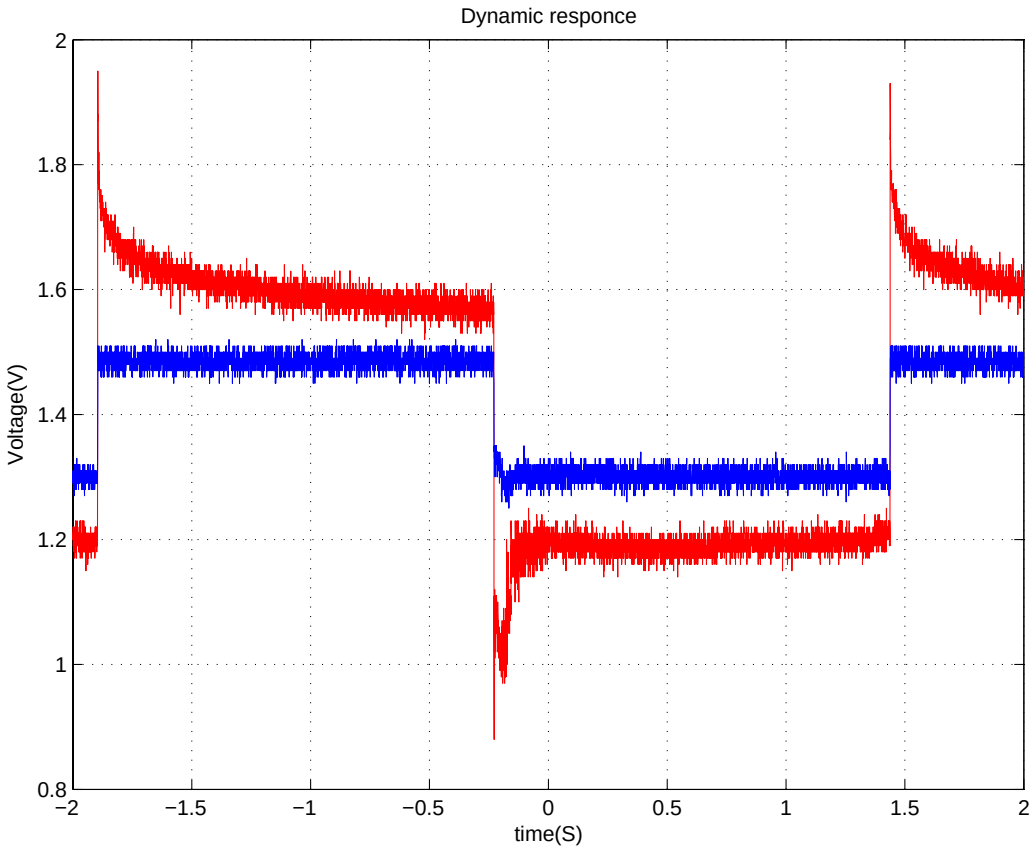

Figure 3.23

This figure shows the test result with a bias of 2.2 volts. With a bias of ca 2.2 volts the jump is avoided.

3.7 Bump circuit

Outputs of the Motion detector circuit, VREF and VOUT, produce a voltage compared to each other when illuminated. That voltage can be positive or negative dependent of the change in light intensity. In order to rectify and digitalize that voltage, a bump circuit [31] together with a transistor is used.
The bump circuit is basically made of a differential pair and a current correlator. The input is the differential voltage $\Delta V = V1 - V2$ and the output is *Iout* (see figure 3.24). When the differential voltage ΔV is near zero, the differential pair will divide the bias current through $Q7$ equally between $Q1$ and $Q4$, thus a current will flow to the output through $Q2$ and $Q3$ due to the current mirrors and *Iout* will have its maximum value. If ΔV is different from zero by a few units of kT/q, the differential pair will force all the current to flow through one of it's legs, thus one of the output transistors($Q2$ or $Q3$) in the middle branch shuts off and *Iout* will drop to zero. $Q2$ and $Q3$ are connected in series and act as a sort of analog logical $\overline{XOR}$ combination. This behavior is displayed in figure 3.24 B.

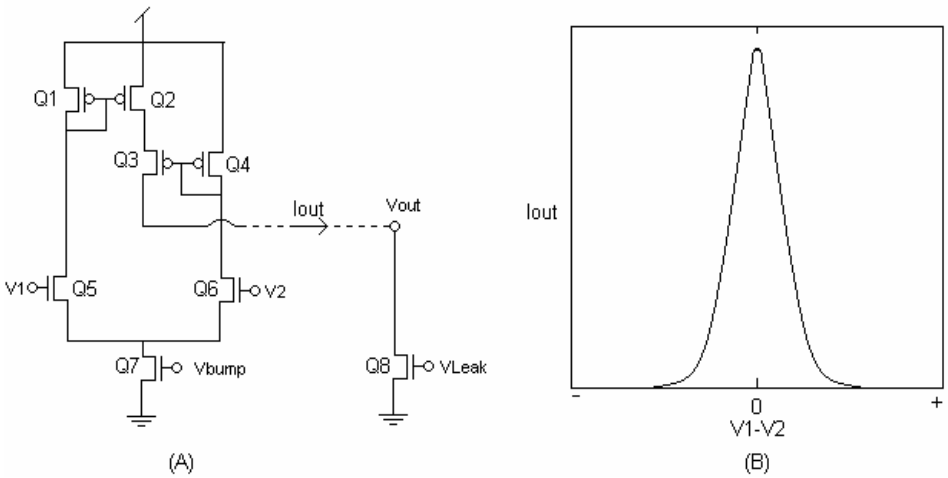

Figure 3.24

The output of the bump circuit is an analog current that is proportional to the $|\Delta V|$ and to convert that current to a sharp digital transition, a biased transistor $Q8$ is connected between the output of the bump circuit and ground. If the output current of the bump circuit becomes smaller than the bias current through $Q8$, the drain voltage of $Q8$ will drop, and if the output current is larger than bias current through, $Q8$ the drain voltage of $Q8$ will rise to ca vdd.
The sensitivity of this change detection mechanism can be regulated by balancing the current of the bump circuit through $Q7$ and the bias current through $Q10$.

Component sizes of the bump circuit.

Component	Width	Length
Q1	**2**	**1**
Q2	**1.8**	**1**
Q3	**2**	**1**
Q4	**2**	**1**
Q5	**2**	**1**
Q6	**2**	**1**
Q7	**2**	**2**
Q8	**2**	**1**

Table 7

Buffer

To make the output pulses sharper and adjust the load impedance, circuit below was used as a buffer. The buffer consists of 1 differential OPAMP and 2 inverters as shown in figure 3.25. The second inverter in the cascade is made larger than the first one to be able to drive larger loads.

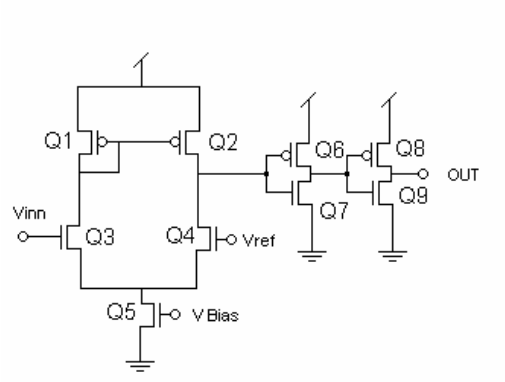

Figure 3.25

The bias *Vref* able us to adjust the sensitivity of the circuit by choosing the operating point. V Bias decides the amplification of the op-amp.

Component sizes of the buffer.

Component	Width	Length
Q1	**2**	**1**
Q2	**2**	**1**
Q3	**2**	**1**
Q4	**2**	**1**
Q5	**2**	**2**
Q6, Q7	**0.8**	**0.35**
Q7, Q8	**2**	**0.35**

Table 8

The test result from a dynamic pixel is shown in figure 3.26.

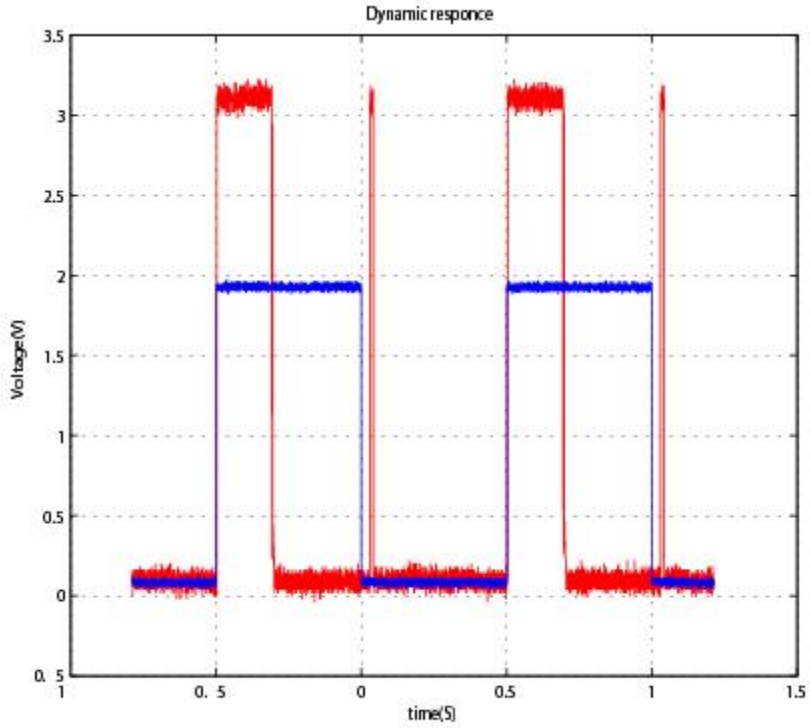

Figure 3.26

The blue line is the voltage on the input resistance in series with a blinking LED placed 10 cm from the cell. The reaction of the circuit is shown as the red graph. From the figure we see that when the input rises, the circuit reacts instantly and drops to zero after a short time, but when the input goes low, the circuit reacts with a delay. This delay is because of the asymmetric NLE properties discussed in chapter 3.5.

For an idea of the system response of the dynamic pixel we measured the cut off frequencies versus stimulus amplitudes. Figure 3.27 shows that the circuit's cut-off frequency increases linearly with the light intensity. The lowest frequency is hard to fine as the circuit responded to very low frequencies as 0.1 Hz. The highest frequency was also difficult to measure, because of the limitations with the light diode.

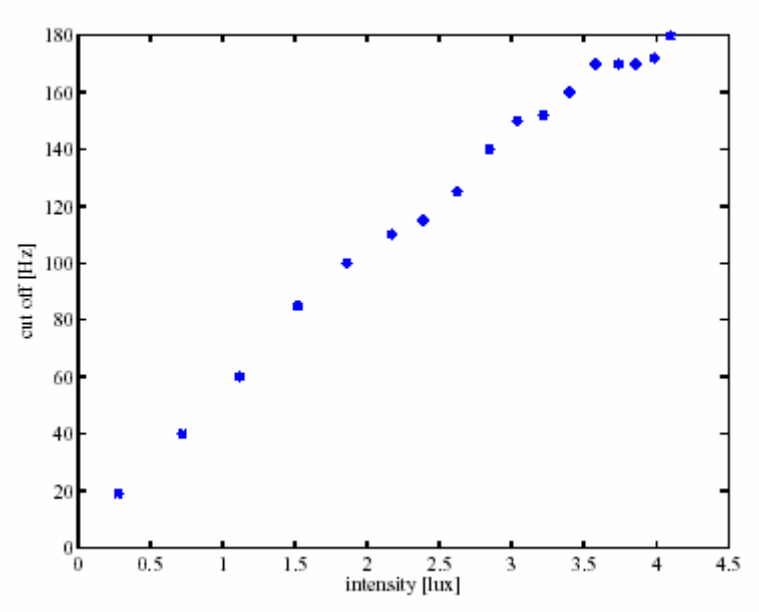

Figure 3.27

Light intensity versus cut-off frequency, The X-axis is the light intensity in lux and the Y-axis is the measured cut-off frequency of the circuit.

Layout of the dynamic pixel.

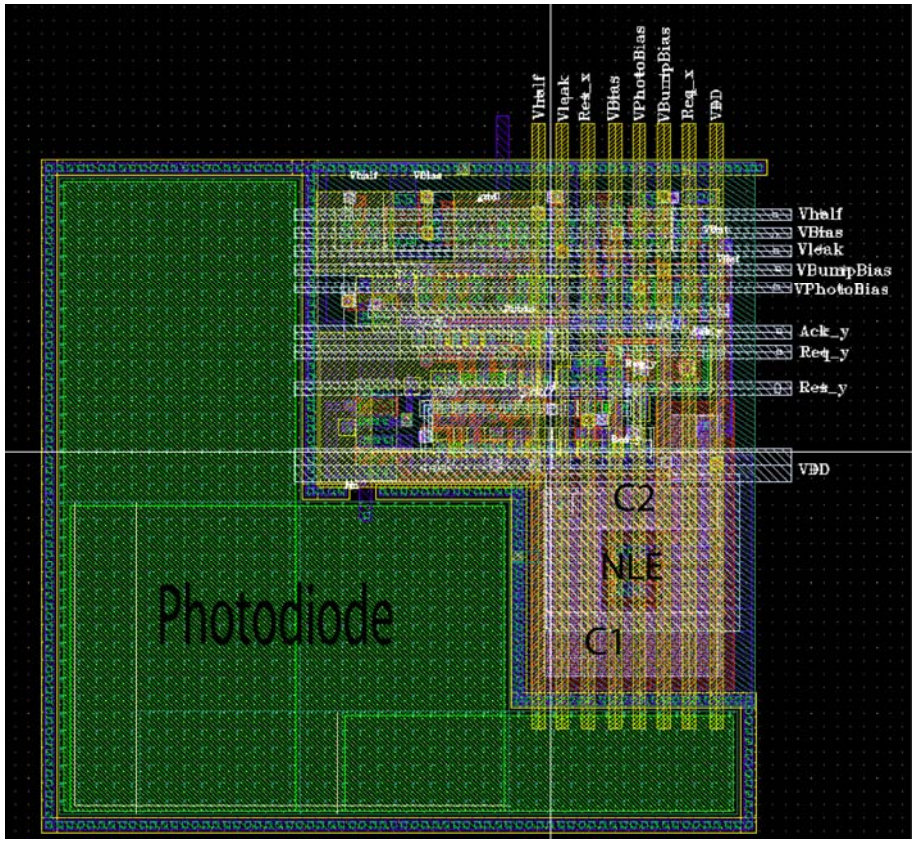

Figure 3.28

Figure 3.28 shows the layout of the dynamic pixel. A big part of the cell consist of photodiode to achieve maximum light sensitivity. Address and supply lines connecting the pixel to the periphery circuitry and other pixels are crossing the photodiode making the effective fill factor to be smaller than the size of the photodiode. Each pixel is surrounded by GND guard to achieve good noise properties.

3.8 Communication and the AER

To avoid collisions in the AER when two or more pixels fire at the same time, the circuit below is used.

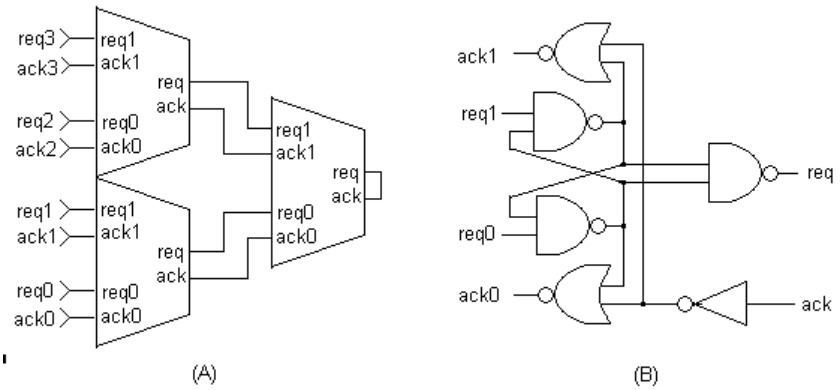

Figure 3.29

The two coupled NAND gates can be looked at a RS flip-flop with active low inputs, see figure 3.29 (B). Normally if there is no request, this RS flip-flop is in its 'illegal' state when R and S are set. Both outputs will be forced to 1. Which state the flip-flop will fall into is determined by which of the two inputs, S or R, is withdrawn first. Or in other words which active high request ('req0' or 'req1') comes in first. If req0 is the winner, then the output of the lower NAND gate will become 0 and the signal 'req' will be propagated to the next layer of the tree. If that 'req' is granted by an incoming 'ack', 'ack0' is set. Following a four phase handshake protocol the requesting instance will thereupon withdraw its 'req0'. If in the meantime 'req1' has been set, that request gets also granted without releasing 'req'. That principle of serving all local requests first before giving control back to the higher level in the hierarchy is called *greedy arbitration*. Only if there are no more request from the left ('req0' and 'req1') is 'req' withdrawn and other arbiter cells on the same level get a chance of being acknowledged.

These arbiter cells can be assembled into a binary tree, see figure 3.29 (A). The top most 'ack' and 'req' can be shorted together.
The disadvantages of this type of collision handling are that some signals can be delayed. The system is also unfair, neighboring pixels get priority over more distanced pixels. On the other hand no signal will be lost in this system.
In the static pixel, the active low signal from the I&F is first inverted to activate $Q1$ and $Q2$. See figure 3.21. To achieve bus access, $Q1$ sends first a request to the right side of the arbiter by pulling REQ-Y low and when the bus is available, the arbiter acknowledges that request by sending a 1 to ACK_Y. $Q2$ and $Q3$ will then send a request to the x-arbiter on top by pulling the REQ_X low. The peripheral AER circuitry completes an off chip communication, sending the pixels address, and then asserts the two reset signals (RES_X and RES_Y) to reset the pixel (see page 56 for more details).

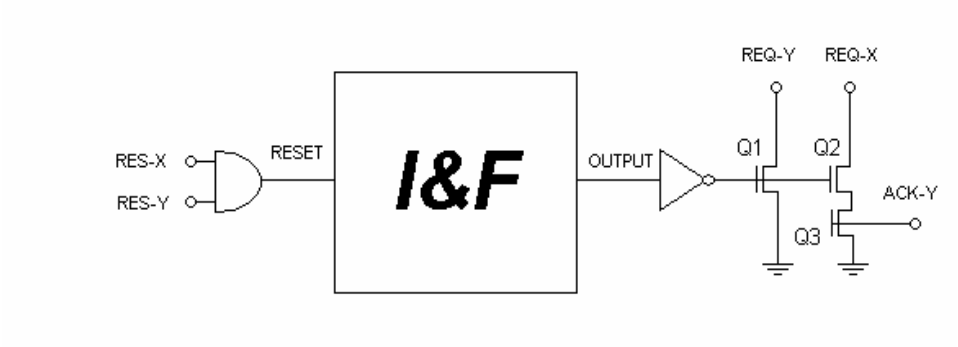

Figure 3.30

In the static pixel the I&F circuit acts as a latch and the output signal is kept until a reset is asserted from the arbiter.

The same communication system is used in the dynamic pixels. In addition to the pull down transistors, a latch is used to detect and hold the output value of the dynamic pixel, see figure 3.31. The latch is a positive edge trigged flip-flop. The reset signals from the arbiter are connected to the clear (CLR) input of the latch through a AND gate.

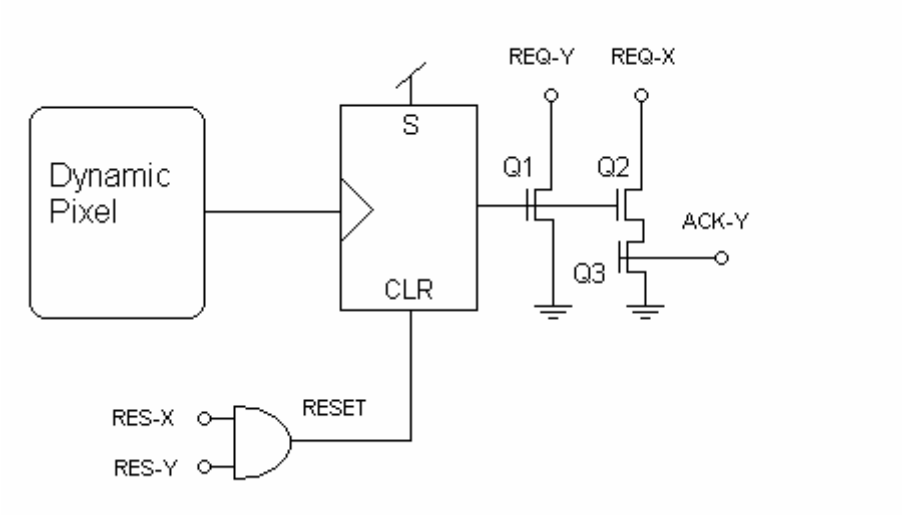

Figure 3.31

4. Conclusion and Proposals

In this thesis we have presented a neuromorphic foveated AER imager chip that shares some functionalities with the retina in the human eye. In the centre of the pixel array we have sharp vision and in the peripheries motion detection. Each pixel decides individually when to fire an AP due to illumination, independent of the read out technology. Using the AER to read out the data from the pixel array, makes the circuit fast and gives us the advantage of low power consumption. That is certainly the case for the dynamic pixel in our design, since they only detect the edge of a moving object and thus a few of the pixels will be active at the same time. The imager is highly effective if for example used as a remote surveillance, where power efficacy and compactness is important. Using an external wake up mechanism to activate the static pixels (opening the electrical shutter, voltages on $V1$ and $V2$) if a motion is detected by the motion detectors, makes the circuit even more power conservative. The imager can also be used in robots, giving them a visual sensitivity with some of functionality as in the human eye.

Both pixel types take advantage of mixing analog and digital technology to achieve high performance and low space consumption. In the dynamic pixel motion is detected in to an analog voltage change and then digitalized using a bump circuit. The I&F circuit in the static pixel is basically a simple, but smart mix-mode circuit that performs analog to digital conversion without any external circuits. Designing these circuits as pure digital, would have resulted in precise but large circuits with huge power dissipation.
Measurements on the imager showed that the imager work as expected, except some problems with offset in the static pixels. These types of offset are almost impossible to avoid mainly because of the mismatch between transistors in the current mirrors and mismatch between the photodiodes. These mismatches in the static pixel resulted in so called salt and pepper noise that was clearly observed in pictures taken by the imager. The MonteCarlo simulation appendix C revealed that the I&F can produce pulses with variations in the frequency due to parameter and process mismatches. This is one of the sources of the noise in the circuit, but not noticeably, because the firing rate of the I&F is also limited by the AER as the I&F needs to be reset by the AER before it can start producing a new pulse.
The oscillations in dynamic pixels results in false APs that can be received as motion by a receiver, but as these APs are produced due to a change in light, they can be spotted and ignored, this phenomenon was only observed in transition from light to completely dark.

This circuit is a prototype experimentally fabricated in a CMOS 0.35 μm CUP process. Most of the transistors in the circuits were made wide and long, this to avoid mismatch and leakage, as a result the pixels became larger, giving a lower resolution to the imager.
The imager shows circuits based on the biology are fully functional and can compete with the best digital circuit available today, sometimes with better results. Neuromorphic circuits may in future become a substitute for today's well developed digital systems, but much work needs to be done.

4.1 Future Work.

Research on neuromorphic circuits is in its beginning, and much work remains before circuits that can compete with the best digital circuits are designed and produced. The imager presented in this thesis works, but is still a prototype that needs to be worked on. Some of the future works that can be done on the imager to increase its performance is listed below.

- Improve the static pixels noise properties to achieve more uniform pictures.
- Produce smaller static pixels to achieve high resolution pictures.
- Static pixels that detect colour.
- Have a connection between the pixels, as in the cells in the human eye.

A. PUBLICATIONS

A FOVEATED AER IMAGER CHIP

M. Azadmehr, J. P. Abrahamsen and P. Häfliger

Institute of Informatics, University of Oslo, Norway
e-mail mehdia@ifi.uio.no, hafliger@ifi.uio.no

ABSTRACT

We have developed a foveated imager chip with high resolution photo-cells (referred to as static pixels) in the center that are surrounded by more space consuming adaptive change detection pixels (referred to as dynamic pixels). Inspired by the neurons of biological nervous systems, they emit short voltage pulses, the static pixels with a frequency proportional to light intensity, the dynamic pixels whenever they detect a relative change in irradiance. The pulses are transmitted off-chip by the Address Event Representation (AER) protocol, i.e. via a digital bus as the identifying address of the sending pixel. For the motion pixels, this read-out strategy has the advantage of low latency in the order of 100ns after a change is encountered. (Whereas a scanning read-out strategy would on average suffer a delay of half of the frame scanning period.) Mounted on a pan-tilt system the peripheral motion detectors could, for instance, be used to steer the imager such that the image of a moving object falls onto the central pixel array where it can then be examined in detail at a higher resolution. Or if the imager is mounted statically they can detect an intruder and cause the central pixels to be turned on for more detailed observation.

1. INTRODUCTION

The eye of human beings is quite differently organized than today's digital cameras. For one thing, the sensory cells in the retina at the back of the eyeball do not merely record an image, but they already process it before it is conveyed to the brain. The photo-receptors perform temporal and spatial filtering. Since the nineties this has also been introduced into a number of 'intelligent' silicon imagers, such as the silicon retina [1, 2].

Furthermore, the nature of the processing in retinal photocells is changing with the location relative to the center of the visual field: Close to the center, the so called Fovea, more details of the unprocessed image are faithfully recorded and passed on to the higher level nervous system for processing, whereas in the peripheral vision the spatial resolution and the colour resolution is rather bad but the cells are very sensitive to minimal changes in light level. This has recently been adapted into so called 'foveated' imagers with, for instance, resolution changing with distance from the center [3–5].

The means by which the visual information is then passed on for further analysis and processing is also very different. In the retina, in every 'pixel' ganglion cells convey the gathered visual information of the whole visual field in parallel as pulse streams. This form of pulse communication by dedicated point to point connections is the general method of communication between nerve cells. A method to emulate this in electronic devices, despite the fact that real point-to-point connections of a density comparable to the one in the nervous system is far out of reach for integrated circuits, is address event representation (AER) [6, 7]: In short, the superior speed of electronic systems is traded in for the inferior cable density. Every pulse emitter is given an identifying 'address'. Whenever it wants to send a pulse, its address is placed on a common digital bus. Receiving sites observe that bus and are triggered if the address of the corresponding sender appears. One such pulse transmission takes in the order of 100ns [8] and thus, although real parallelism is lost, some 100 nano seconds time difference is still virtually simultaneous on the time scale of biological signals (one neuronal pulse (called action potential) lasts for about 1ms and neurons in general fire with a maximal frequency of less than 200Hz).

2. METHODS

The foveated imager chip presented here contains two types of photo cells that will be referred to as static pixels and dynamic pixels in the following. The pixel array is made up of 70x67 static pixels in the center and it is surrounded by four rows of dynamic pixels on all sides (616 dynamic pixels in total). Both circuits communicate by short voltage pulses that are conveyed off chip by AER. The static pixels emit pulses at a frequency that is proportional to the light intensity. The dynamic pixels are sensitive to minimal changes in intensity and emit a single pulse when that change exceeds a certain speed- and and magnitude-threshold. A photo diode is used as the light sensitive component in both circuits. The prototype imager chip has been produced in 0.35μm AMS CMOS technology and measures 3150x 3150 μm, including the padframe.

2.1. Static Pixel

The static pixel is depicted in figure 1. A photo diode emits a current that is proportional to the light intensity. That current is then amplified linearly by a current mirror. The gain can be regulated by the source voltages V_1 and V_2 and can be expressed by the following equation (ignoring effects of the slope factor)

$$\frac{I_{out}}{I_{in}} = e^{\frac{V_1 - V_2}{U_T}} \quad (1)$$

This work was supported by the EU 5$^{\text{th}}$ Framework Programme IST project CAVIAR.

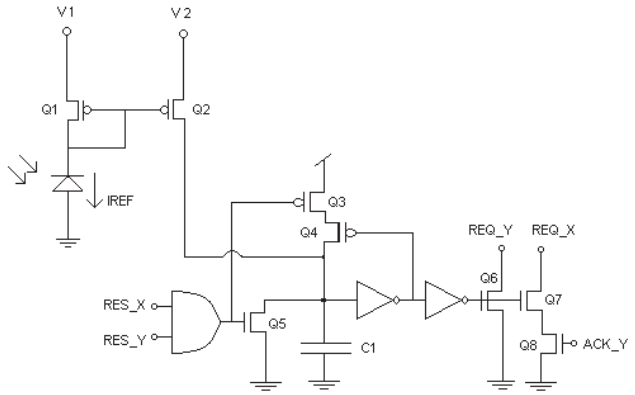

Figure 1: *Schematics of the static pixel*

This conveniently allows to control the amplification by a bias from off-chip, and thus, offers an 'electronic shutter' function, that can be used to tune the central array to different light levels, or to turn it on and off.

Current from the current mirror charges capacitor C1. When the voltage on C1 reaches the digital switching threshold, the first inverter's output goes low, activating Q4 and stabilizing the voltage on C1 at Vdd. The second inverter's output going high triggers a request to the AER arbiters on the periphery of the pixel array. (Please refer to [8] for more details on the AER communication.) A request for bus access is sent to the y-arbiter on the right by pulling REQ_Y low, and if acknowledged (ACK_Y going high) a request is made to the x-arbiter on the top by pulling REQ_X low. The peripheral AER circuitry then completes a off chip communication, sending the pixel address, and then asserts the two reset signals (RES_Y and RES_X) that reset the pixel. The frequency of these address events from a pixel is, thus, proportional to the photo current.

The static pixel measures 26.8 x 25.2 μm and has fill factor (light diode area) of 11.3%

2.2. Dynamic Pixel

The Dynamic pixel is shown in figure 2. It consists of three main blocks. The first block (A), is the adaptive photo cell designed by T. Delbrück [9]. This circuit has high-pass properties, adapts to the time average light level and amplifies small changes in light logarithmically. Its ability to adapt to a large range of light intensity, allows the dynamic pixel to function without need of a shutter over a large range of illumination levels. The intended output of the adaptive photo cell is the voltage V4, but the amplified small changes can also be observed as a voltage difference between V3 and V4. In our design, V3 and V4 are connected to a bump circuit (in block B) [10] that is used to rectify the voltage difference. The output current of the bump circuit becomes smaller with increasing difference of the input voltages. If it becomes smaller than the bias current through Q11, the drain voltage of Q11 drops and is amplified to a sharp digital transition. The sensitivity of this change detection mechanism can be regulated by balancing the current through Q11 and the bias current of the

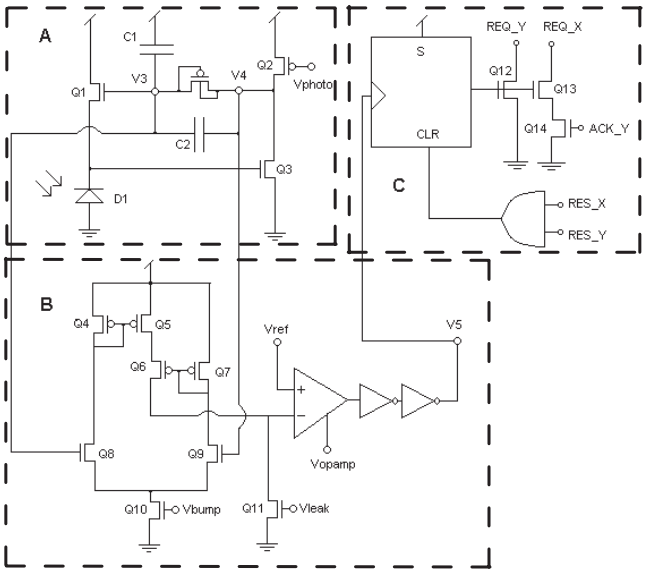

Figure 2: *Schematic of the dynamic Pixel*

Vphoto	1.2V	Vleak	0.2V
V1	3.19V	Vopamp	0.7V
V2	3.3V	Vref	1.2V
Vbump	0.42V		

Table 1: *Parameters used for the measurements presented in the paper, unless stated explicitly*

bump circuit through Q10. The rising transition in the output voltage of the double inverter sets a latch (in block C) that then is used to initiate a requests to the AER arbiter, in the same way as described for the static pixel. The latch is reset asynchronously at the completion of the communication.

One dynamic pixel occupies an area of 53.6 x 50.4 μm and has a fill factor of 50.4 %.

3. RESULTS

The response of the individual pixels has been tested in a dark room by using a red light emitting diode (LED) placed 10 cm from the chip without lens. We supplied a voltage across the LED with a resistor in series. The light intensity of the LED is roughly proportional to the current and thus to the voltage across the serial resistor. However, we corrected that assumption somewhat for all the figures by measuring the irradiance in the position of the chip with a Lux meter[1].

3.1. Static Pixel

When testing the static pixels, the average frequency of all 70x67 static pixels was recorded. Results are shown in figure 3. The two curves (diamonds and asterisks) are obtained with different settings for amplification in the current mirror.

[1]Lux here is the measure for irradiation, corrected for the wavelength spectrum of human vision. 1 Lux of red light of 650nm wave length corresponds to an irradiance of 0.015 Watts per square meter

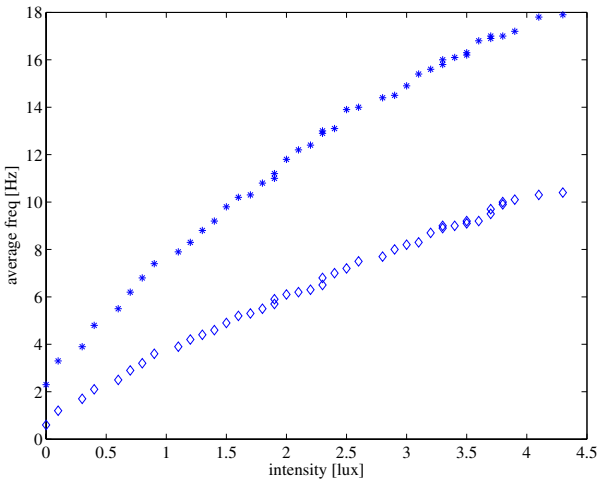

Figure 3: *Average pulse frequency of the static pixels versus light intensity in lux for two parameter settings*

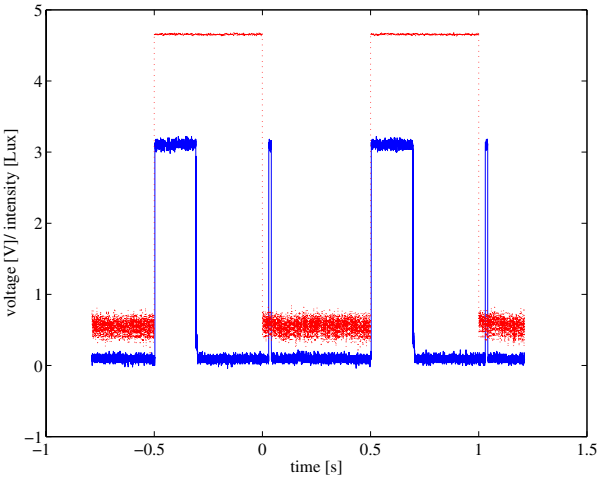

Figure 4: *Solid curve: response of an individual dynamic pixel in volts (V5 in figure 2);dotted curve: stimulating light intensity in Lux*

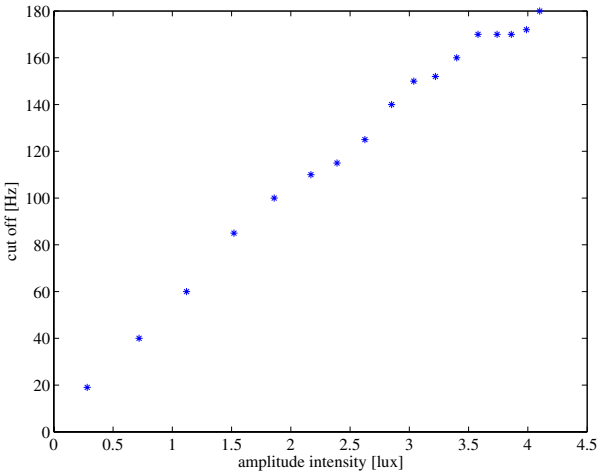

Figure 5: *Stimulation frequency beyond which the dynamic pixel ceased to respond versus input amplitude*

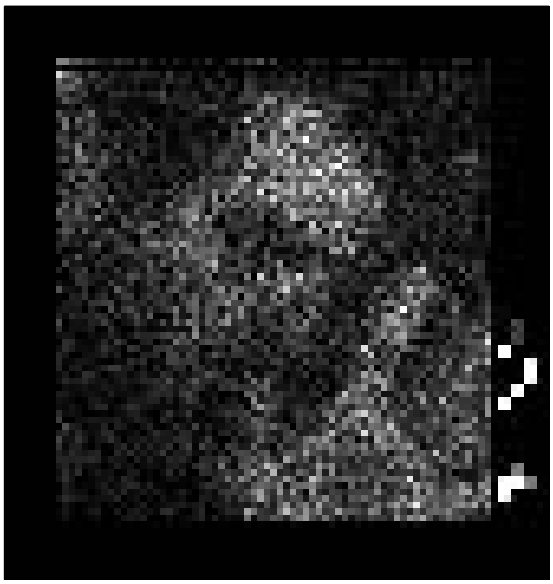

Figure 6: *An image from the whole array. On the right, the person in the field of view is waving his hand, activating the peripheral dynamic pixels.*

Average firing frequency versus illuminance is shown. At the lower amplification (V1=3.19V, diamonds), the curve is approximately linear. At the higher amplification (V1=3.16V, asterisks) the curve starts to show effects of saturation. This is due to over-running of the AER receiver that was used to read out the pixel pulses. We used a digital data acquisition PCI card to sample the bus (including the request and acknowledge of the 4 phase handshake that were shorted together) at a frequency of 1.25MHz. By processing in software we would then scan for positive transitions of the request signal to identify an address event. By voltage biases of the AER block on the chip the transmission rate was artificially slowed down, such that the positive phase of the shorted request/acknowledge signal would last about 1μs, enough for it to be detected during a 0.8μs sampling interval. The interval between such pulses, however, could not be forced to be longer than a few tens of nanoseconds, if several communications were pending. Thus positive transitions of the request signal started to be missed by the recording device as the bus started to be crowded. This effect became more pronounced the higher the average output frequency, until it would saturate at about 24Hz. This problem would, however, not occure at these low frequencies with a faster receiver.

With adjusted amplification the static pixels would also operate satisfactorily with normal indoors illumination (up to some 100 Lux). Due to the exponential tuneability of the amplification we expect it to work in broad daylight as well. The later was not tested though due to the bulky measuring setup.

3.2. Dynamic Pixel

A single dynamic pixel outside the array was tested by using the same test setup as for the static pixels. The LED's supply voltage was now controlled by a function generator, at first supplying a square wave voltage resulting in illumination

levels switching between almost zero up to 4.6 Lux, i.e. almost 100% contrast. (see figure 4, dotted curve). A positive transition of the dynamic pixel (solid curve, voltage V5 in figure 2) indicates the detection of a change. The delay of the response for the negative change is rather big and the pulse shorter. That is on one hand due to the asymmetric nature of the non-linear element in the adaptive photo cell, on the other due to the logarithmic nature of the adaption: When adapted to a low light level, changes have a bigger effect.

When a sine wave stimulus was used instead, the pixel response would sometimes not be a clear digital pulse but oscillate at the pulse onset and offset (not shown). This does, however, not diminish the pixel's ability as a change detector.

For an idea of the system response of the dynamic pixel we measured the cut off frequencies versus stimulus amplitudes (see figure 5, with V_{photo}=0.7, V_{leak}=0.48V, V_{ref}=1.6V, V_{bump}=0.58V). A half wave rectified sine wave stimulus was used. The lower cut off frequencies were hard to identify: as it was tried, the circuit was still responding reliably down to frequencies of 0.01Hz for an intermediate amplitude of 3 Lux. The higher cut off is roughly linearly dependent on the amplitude within the intensity range the LED was able to supply. This is expected as the speed of the response of the photo active element is proportional to the current that it generates, which is again proportional to the light intensity. The dynamic pixel worked well also in normal room lighting conditions. We expect the total range of operation to be of the same order as the range of operation of the adaptive photo cell which was reported to span 5 decades in light intensity in [9].

3.3. Imager

An example indoors image recording is shown in figure 6. The person in the picture is waving a hand at the right side of the image, where the response of the dynamic pixels can be seen. Pixel values are integrated activity decaying with 50% per 0.1 seconds. So a steady activity of, for example, 100 Hz would lead to a pixel value of close to 20. Static pixel values are displayed with a linear gray scale from 0 (black) to 16 (white) (i.e. above about 80Hz is white), dynamic pixel values from 0 to 1 (i.e. single events that indicate a change detection are white).

The image also gives an idea of the 'salt and pepper' fixed pattern noise of the static pixels: a problem that certainly would need to be addressed for an industrial product, but which we considered acceptable for a prototype to demonstrate the concept.

4. CONCLUSION

Foveated imager chips of the kind introduced here are mainly useful in applications where real time performance, compactness, and power efficacy are of importance, such as hidden surveillance or space missions. Otherwise one might be better off using two uniform image sensors mounted beside each other.

If pixel activity is sparse, AER to read out imager data is conceptually more power conservative as opposed to frame scanning. That is an advantage for the dynamic pixels: if a monochrome object traverses the field of vision of these change detectors, only the edges of the object trigger a single pulse response. Thus, most of the cells are silent most of the time. Furthermore, once the pixel has detected a change the AER communication itself causes less than 100ns transmission delay [8], which makes this a method that is well suited for real time applications.

The static pixels in the Fovea, however, are usually constantly active. The use of AER read out offers no conceptual power advantage here. However, for an intrusion detection system, for example, their power consumption could be optimized by employing a 'wake-up' mechanism that uses activity from the motion sensors to open the 'electronic shutter' (i.e. the amplification control via bias voltages V1 and V2).

For these simple static pixels AER read out offers yet another advantage, if fast reaction times are essential: the spikes from the pixels can be integrated over a very short time period only, to get a low quality picture quickly. The picture can also be gradually improved (by continuous integration of the spikes) until it is clear enough for a processing algorithm, to take action.

5. REFERENCES

[1] K. Fukushima, Y. Yamaguchi, M. Yasuda, and S. Nagata. An electronic model of the retina. *Proceedings of the IEEE*, 58(12), December 1970.

[2] C. A. Mead and M. Mahowald. A silicon model of early visual processing. *Neural networks*, 1:91–97, 1988.

[3] F. Ferrari, J. Nielsen, P. Questa, and G. Sandini. Space variant imaging. *Sensor Review*, 15(2):17–20, 1995.

[4] F. Pardo, J.A. Boluda, J.J. Perez, B. Dierickx, and D. Scheffer. Design issues on cmos space-variant image sensors. In *Proc. SPIE, Advanced Focal Plane Proc. and Elec. Cameras*, volume 2950, pages 98–107, 1996.

[5] R. Etienne-Cummings, J. Van der Spiegel, P. Mueller, and Mao-Zhu Zhang. A foveated silicon retina for two-dimensional tracking. *IEEE Trans. on Circ. and Sys. II*, 47(6):504–517, June 2000.

[6] M. Mahowald. *An Analog VLSI System for Stereoscopic Vision*, chapter 3, pages 66–117. Kluwer, 1994.

[7] A. Mortara and E. A. Vittoz. A communication architecture tailored for analog VLSI artificial neural networks: intrinsic performance and limitations. *IEEE Trans. on Neural Networks*, 5:459–466, 1994.

[8] P. Häfliger. *A spike based learning rule and its implementation in analog hardware*. PhD thesis, ETH Zürich, Switzerland, 2000. http://www.ifi.uio.no/~hafliger.

[9] T. Delbrück and C. Mead. An electronic photoreceptor sensitive to small changes in intensity. In *Advances in Neural Inf. Proc. Sys.*, volume 1, pages 720–726, 1989.

[10] T. Delbrück. Bump circuits. In *Proceedings of International Joint Conference on Neural Networks*, volume I, pages 475–479, Seattle Washington, July 1991.

B. More about the neurons

NEURONS

Neurons come with different length and shapes, depending on their functionality and structure. There are different ways to classify neurons, the two most obvious ways are based on structure and function, it is important to note that function follows structure. Structurally neurons can be classified as multipolar, bipolar or unipolar, see figure B.1. **Multipolar neurons** are the most common type in the CNS (central nerve system) and usually have numerous dendritic branches and one axonal process, but some neurons completely lack the axon and have only dendrites. **Bipolar neurons** have just two processes, an axon and a dendrite. These neurons are usually acting as receptor cells in some of the sense organs such as the eyes or nose. **Unipolar neurons** have only a single fibre which divides close to the cell body into two main branches (axon and dendrite), and have no dendrites arising directly from the cell's soma. Unipolar neurons are found in ganglia outside the central nerve system.

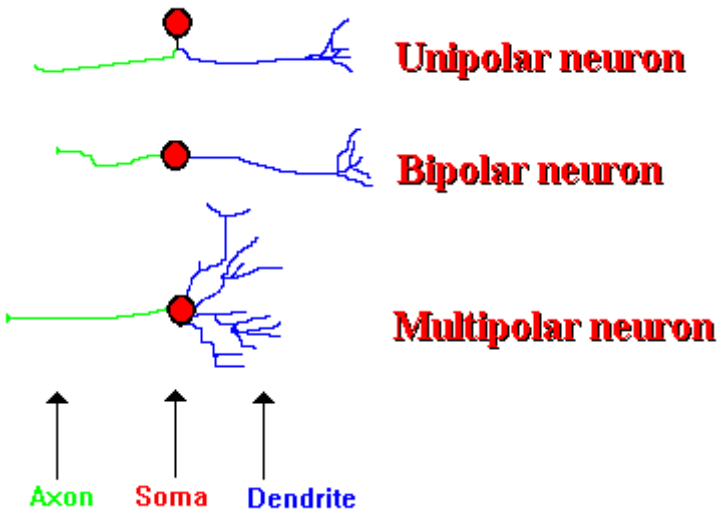

Figure B.1

Functionally there are three types of nerve cell. These are the **sensory neurons**, the **intermediate neurons** and the **motor neurons**. Sensory neurons (afferent neurons) conduct impulses from peripheral receptors to the CNS and are usually unipolar, although some are bipolar neurons. Intermediate nerve cells are multipolar neurons laying within the CNS that form links between other neurons.

Motor neurons are multipolar neurons that conduct impulses from the CNS to muscles [5], [32].

How is an AP produced?

Neurons are surrounded by a semi-permeable membrane that allows some ions to pass through and blocks other ions, this regulation of ions is done by special selective "gates" or "channels". At rest a combination of Cl-, Na+ and K+ give the neuron its resting potential of -70 mV, in this condition the cell regulates the amount of the ions by letting in K+ ions and pumping out Na+ ions. When the neuron receives a stimulus, it creates what is known as a "depolarizing current" by opening the sodium (Na+) channels. There are many more sodium ions on the outside, and the inside of the neuron is negative relative to the outside, sodium ions rush into the neuron. Sodium has a positive charge, so the neuron becomes more positive. If the depolarization reaches about -55 mV a neuron will fire an action potential. If the neuron does not reach this critical threshold level, then no action potential will fire. If the threshold is reached more sodium channels open and the potential rises to 30mV. It takes longer for potassium (K+ ions) channels to open. When they do open, potassium rushes out of the cell, reversing the depolarization. Also at about this time, sodium channels start to close. This causes the action potential to go back toward -70 mV (a repolarization). The action potential actually goes past -70 mV (a hyperpolarization) because the potassium channels stay open a bit too long. Gradually, the ion concentrations go back to resting levels and the cell returns to -70 mV. See figure 1.2.

C. Additional simulations

Motion detector:

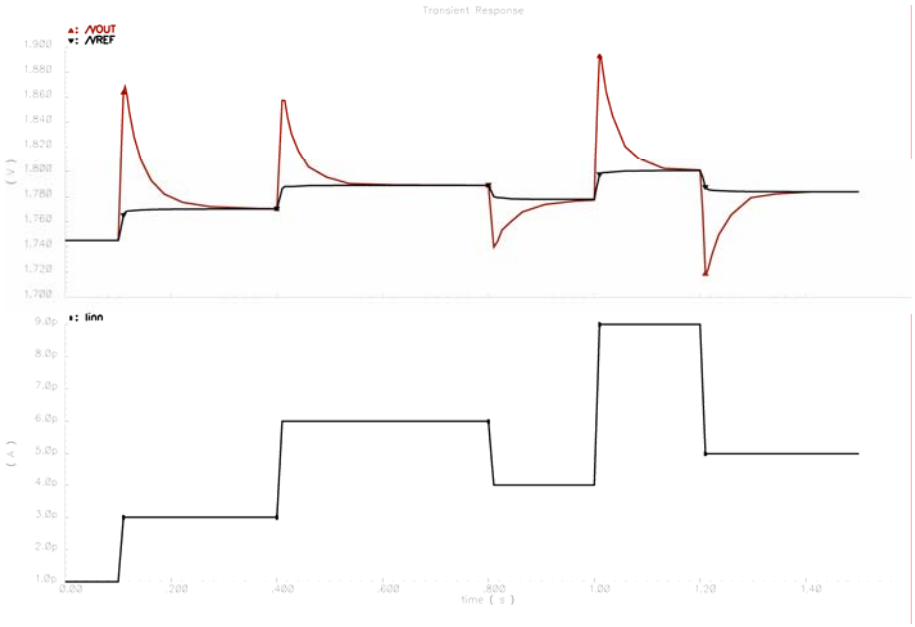

Figure C.1

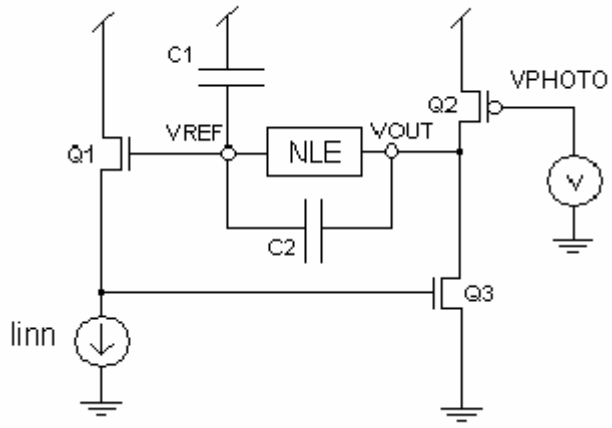

Figure C.2

Figure C.1 shows the simulation result on the circuit shown in figure C.2.
The upper graphs in figure C.1 is the reaction of the circuit to the current changes in at Iinn shown in the lower graph in the same figure. VPHOTO has a value according to table 3.1, (1.2 volts).

Bump circuit:

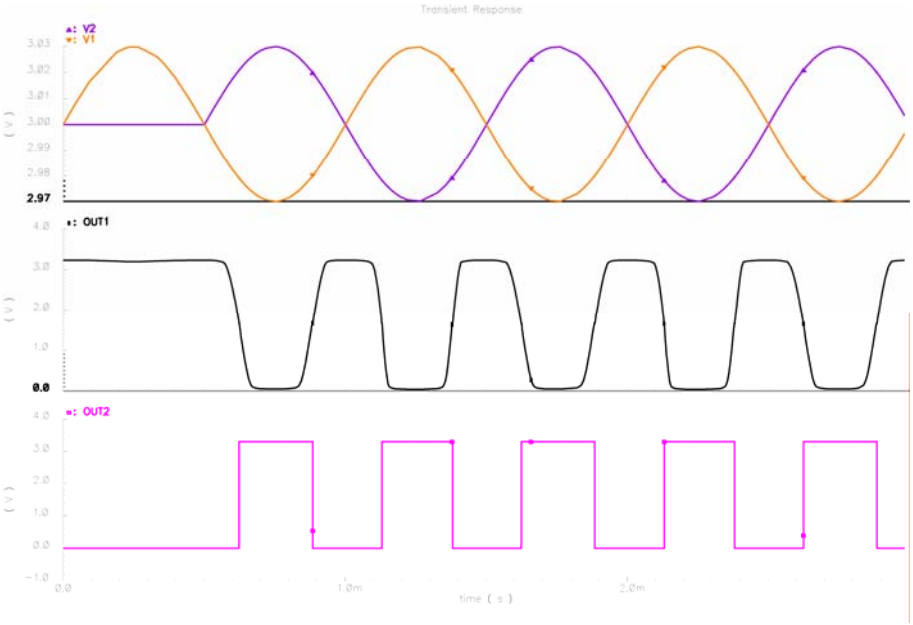

Figure C.3

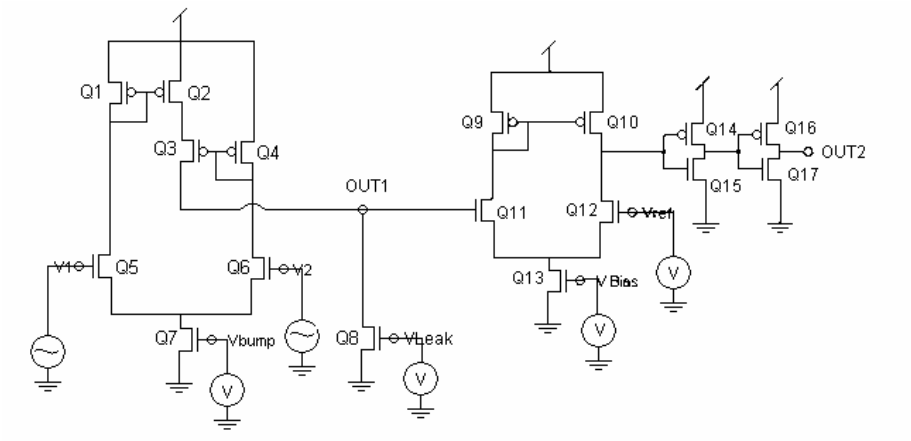

Figure C.4

Figure C.3 shows the simulation result on the circuit shown in figure C.4.
In this simulation we fed the bump circuit with 2 sinus voltages with 180 phase difference oscillating between 2,97 and 3.03 volts. The result is illustrated in the middle graph (OUT1) and the lower graph (OUT2) in figure C.3. OUT1 is the output directly from bump circuit and OUT2 is the result after the buffer. OUT2 is sharper than OUT1.
All the biases have values according to table 3.1 in page 24.

I&F Neuron:

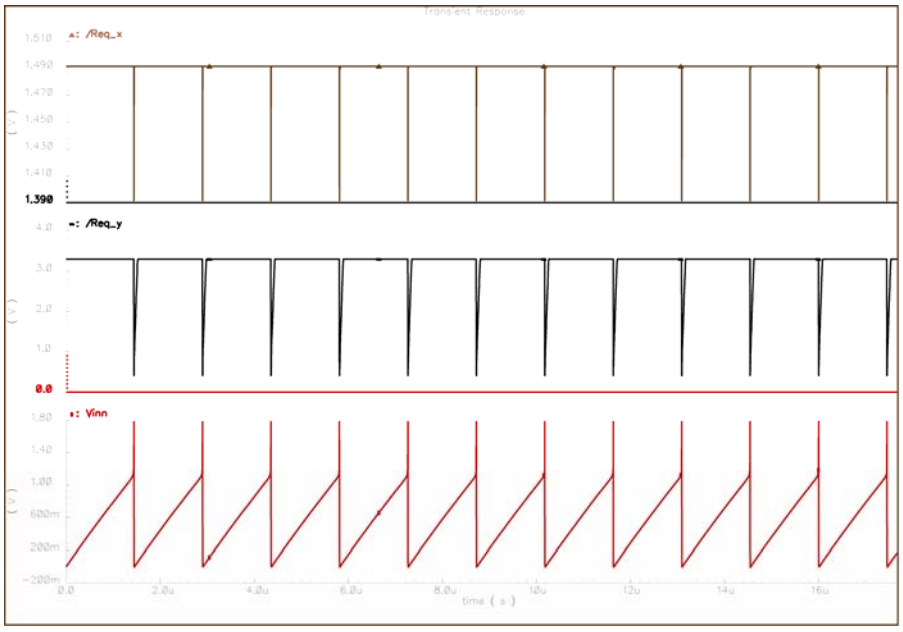

C.5

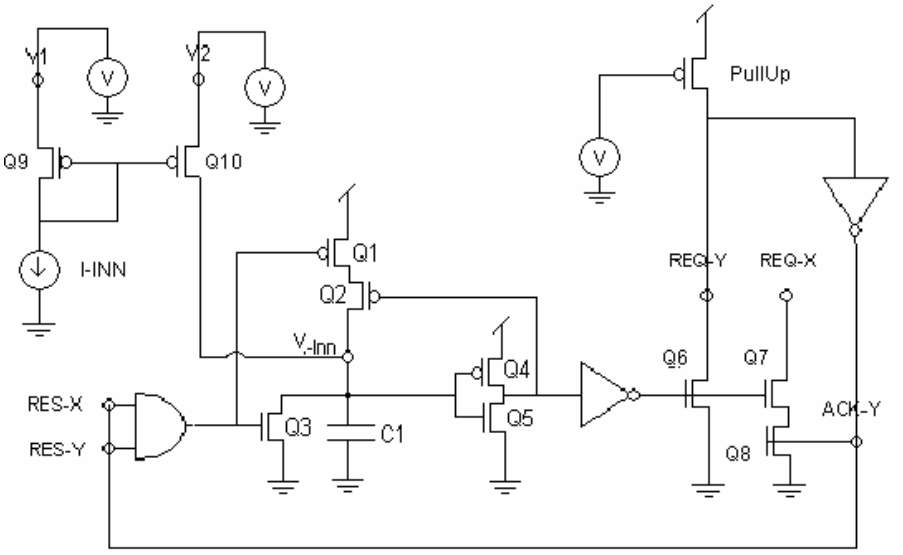

C.6

Figure C.5 shows the simulation result on the circuit shown in figure C.6.
In this test we connected the inverted value of REQ_Y to ACK_Y, reset inputs (RES_X and RES_Y) and fed the circuit with a constant current (I-INN in figure C.6). The lower graph in figure C.5 is the voltage across C1, we can see that V-Inn is rising linearly in the beginning until it reaches the threshold of the following inverter, then it is pulled up by Q2 to a voltage near VDD. The spikes produced by the circuit (REQ_X and REQ_Y) are also illustrated in figure C.5.

MonteCarlo simulation of I&F circuit.

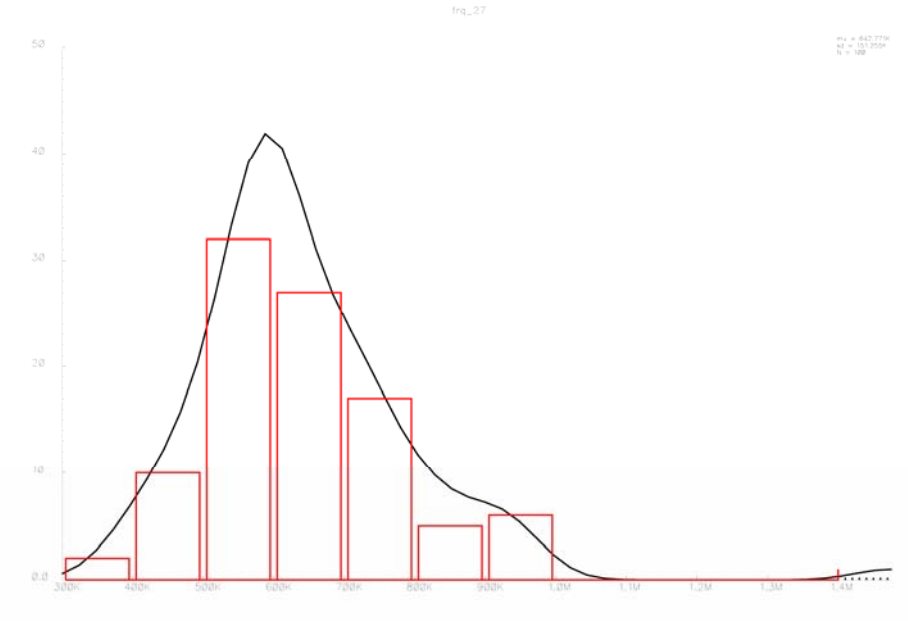

C.7

Figure C.7 illustrates the MonteCarlo simulation of the I&F circuit. This MonteCarlo simulation is generated by 100 simulations with statistical process variations and mismatches. From the graph we can observe a variation of the frequency of pulses generated by the I&F circuit. The graph has its top around 600 KHz with a variation from 300Khz til around 1MHz. This is one of the sources for the salt and pepper noise in the camera discussed in chapter 2.5.

D. Additional Layout and Figures

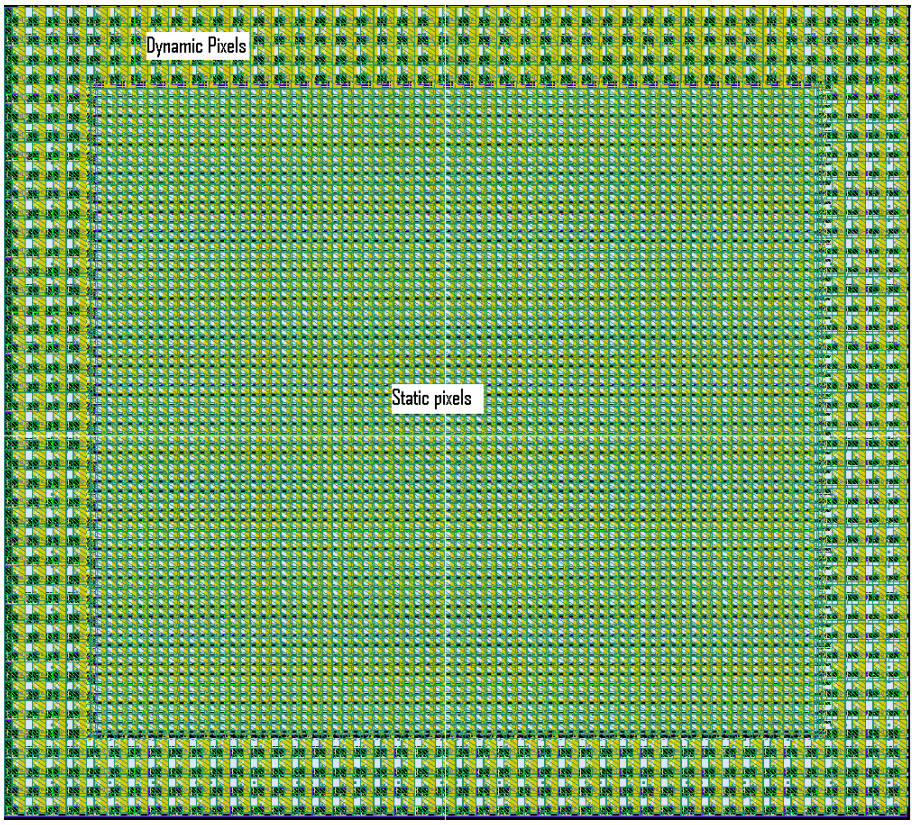

Figure D.1

Figure D.1 shows the pixel-array with static pixels in the middle and dynamic pixels in the periphery.

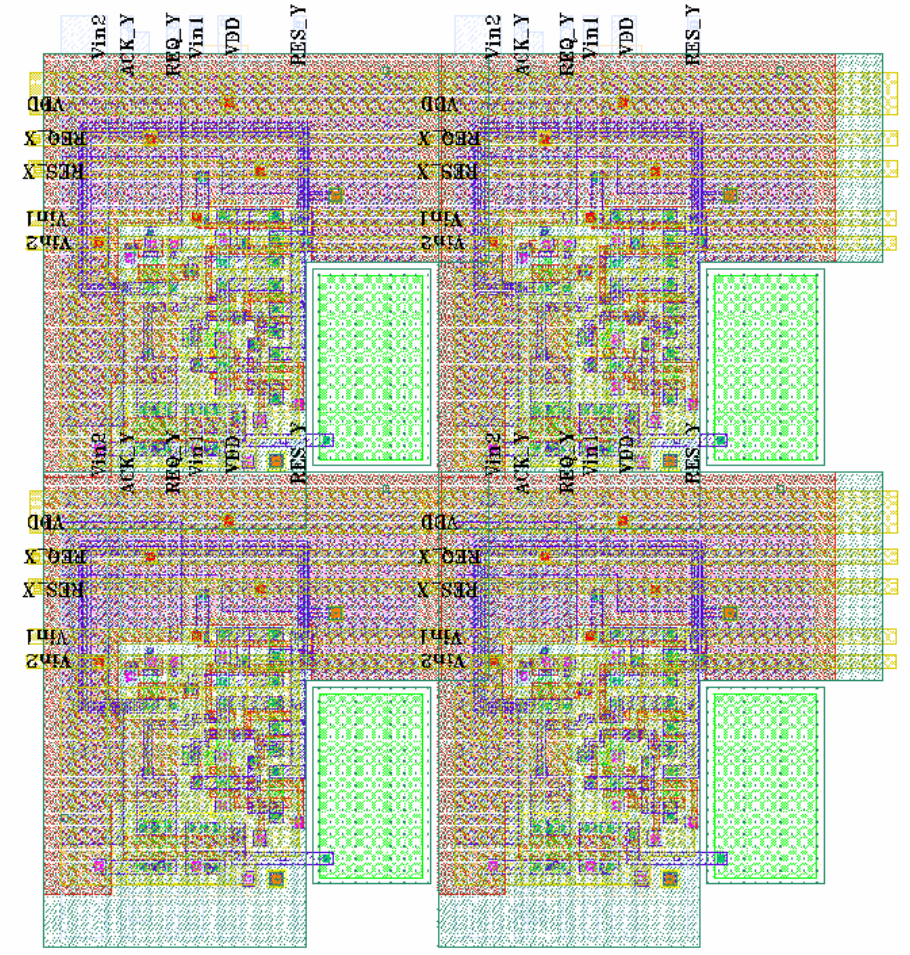

Figure D.2

Figure D.2 shows a 2x2 pixel-array with static pixels.
The communication and supply lines cross the pixels and connect them to neighboring pixels.

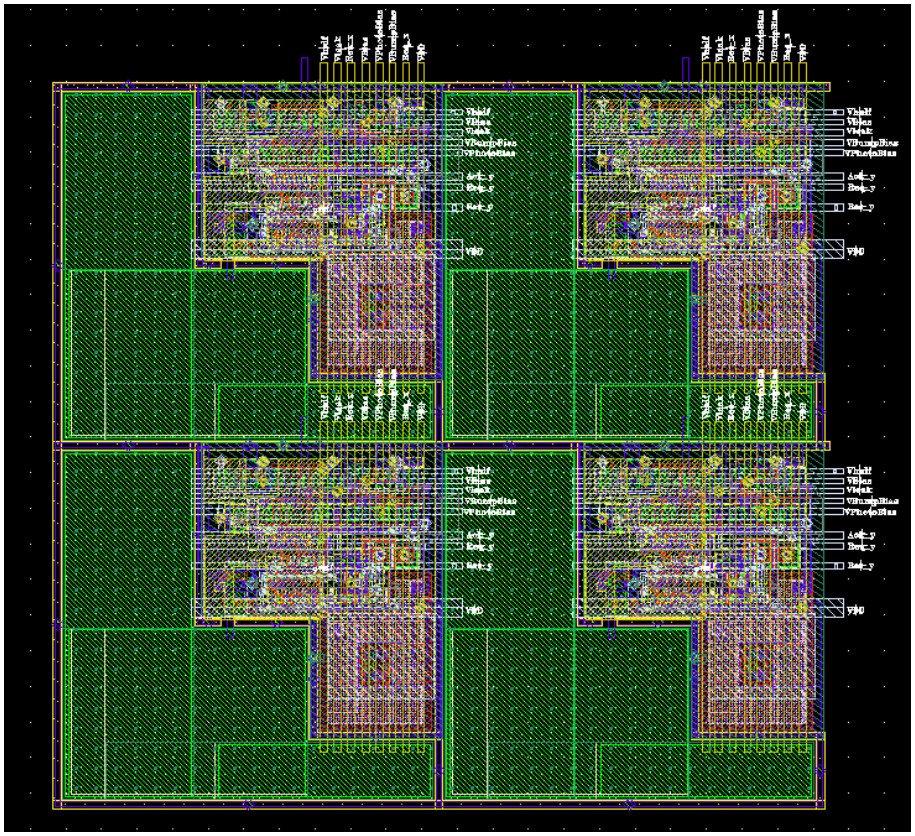

Figure D.3
Figure D.2 shows a 2x2 pixel-array with dynamic pixels.

Bibliography

[1] Hodgkin AL & AF Huxley (1952) The dual effect of membrane potential on sodium conductance in the giant axon of *Loligo*. *J. Physiol.* **116**, 497-506.

[2] C. Mead. ***Analog VLSI and Neural Systems***. Addison Wesley, 1989. Chapter 4.

[3] M. Mahowald and R. Douglas. **A Silicon Neuron**. *Nature*, vol. 354:pp.
515–518, 1991.

[4] www.fortunecity.com
http://www.fortunecity.com/greenfield/buzzard/387/nervecellgen.htm

[5] Instituto de Fisiología Celular, UNAM, Mexico City.
http://ifcsun1.ifisiol.unam.mx/Brain/segunda.htm

[6] Jerry G. Johnson biology homepage
http://www.sirinet.net/~jgjohnso/nervoussystem.html

[7] SÉBASTIEN ROYER AND DENIS PARÉ **Conservation of total synaptic weight through balanced synaptic depression and potentiation** Nature 422, 518 - 522 (03 April 2003); doi:10.1038/nature01530

[8] all about.multiple-sclerosis
http://www.mult-sclerosis.org/actionpotential.html

[9] University of Washington
http://faculty.washington.edu/chudler/ap.html

[10] http://www.tiscali.co.uk
http://www.tiscali.co.uk/reference/encyclopaedia/hutchinson/m0016171.html

[11] S. Thorpe, D. Fize, and C. Marlot. **Speed of processing in the human visual systems.** Nature, Vol.381:pp. 520-522, 1996

[12] **medicinenet.**
http://www.medicinenet.com

[13] **hyper physics**
http://hyperphysics.phy-astr.gsu.edu/hbase/vision/retina.html

[14] **Ted M. Montgomery, O.D**.
http://www.tedmontgomery.com/the_eye/retina.html

[15**] The Washington University School of Medicine**
http://thalamus.wustl.edu/course/eyeret.html

[16]Lecture notes by philipp Hafliger in neuromorphic electronics at UIO
http://www.ifi.uio.no/infneuro/Gamle/H2002/hafliger/retinomorph.html

[17] K. Fukushima, Y. Yamaguchi, M. Yasuda, and S. Nagata. **An electronic model of the retina**. *Proceedings of the IEEE*, 58(12), December 1970.

[18] C. A. Mead and M. Mahowald. **A silicon model of early visual processing**. *Neural networks*, 1:91–97, 1988.

[19] Robert Wodnicki, Gordon W. Roberts, Martin D. Levine, **A Foveated Image Sensor in Standard CMOS Technology,** Department of Electrical Engineering, McGill University, Montr_eal, Qu_ebec, CANADA, H3A 2A7.

[20]1996R. Etienne-Cummings, J. Van der Spiegel, P. Mueller, and Mao-Zhu Zhang. **A foveated silicon retina for twodimensional tracking**. *IEEE Trans. on Circ. and Sys. II*, 47(6):504–517, June 2000.

[21] F. Ferrari, J. Nielsen, P. Questa, and G. Sandini. **Space variant imaging. Sensor Review**, 15(2):17–20, 1995.

[22] Giulio Sandini (1), Paolo Questa (2), Danny Scheffer (3), Bart Dierickx (3), Andrea Mannucci *(4).** **A retina-like CMOS sensor and its applicatins** IEEE SAM Workshop, March 16-17, 2000, Cambridge, USA

[23] F. Pardo, J.A. Boluda, J.J. Perez, B. Dierickx, and D. Scheffer. **Design issues on cmos space-variant image sensors.** In *Proc. SPIE, Advanced Focal Plane Proc. And Elec. Cameras*, volume 2950, pages 98–107,

[24] Master Thesis: Jens petter Abrahamsen, **Neoromorft kamera,** university of Oslo

[25] Larry Godfrey, **Choosing the Detector for your Unique Light Sensing Application,** PerkinElmer, Inc.

[26] M. Mahowald. ***An Analog VLSI System for Stereoscopic Vision***, chapter 3, pages 66–117. Kluwer, 1994.

[27] A.Mortara and E. A. Vittoz. **A communication architecture tailored for analog VLSI artificial neural networks: intrinsic performance and limitations**. *IEEE Trans. On Neural Networks*, 5:459–466, 1994

[28] P. H¨afliger. **A spike based learning rule and its implementation in analog hardware**. PhD thesis, ETH Z¨urich, Switzerland, 2000. http://www.ifi.uio.no/˜hafliger.

[29] **Electonic Devices**, Fifth Edition, Thomas L. Floyd. Prentice Hall

[30] T. Delbrück and C. Mead. **An electronic photoreceptor sensitive to small changes in intensity**. In *Advances in Neural Inf. Proc. Sys.*, volume 1, pages 720–726, 1989

[31] T. Delbrück. **Bump circuits**. In *Proceedings of International Joint Conference on Neural Networks*, volume I, pages 475–479, Seattle Washington, July 1991.

[32] The University of the Western Cape, The Department of Biodiversity & Conservation Biology.
http://www.botany.uwc.ac.za/sci_ed/grade10/mammal/nervous.htm